

CHAPTER TWO

CHEMICAL REDUCTION METHODS

2.0 INTRODUCTION

The most widely used method for the synthesis of gold nanoparticles (AuNPs) is the reduction of a gold salt. This method requires a reducing agent in the presence of a capping agent for the formation of surface passivated gold nanoparticles [1]. Many methods have been used to improve the quality and control the physical properties of gold nanoparticles. A major goal of these methods is to produce high quality nanoparticles in a monodispersed form (i.e. with uniform/controllable size, shape and coefficient of variance) because the size and distribution of the particles are important factors that determine their physical and chemical properties [2]. It is generally believed that the current and potential applications of nanostructured materials are dependent on those properties. For example, the use of thiols, polymers, surfactants and other ligands control particle size, shape and also prevent agglomeration. They can also introduce functionality to the surface of gold nanoparticles, an important feature for applications in nano-biology [3,4].

The citrate reduction of HAuCl_4 in water, first reported by Turkevitch *et al.* is a well known method for the synthesis of AuNPs [5]. Nanoparticles produced by this technique are approximately 20 nm in size. The size of such nanoparticles is controlled by varying the stabilizer to gold ratio. The possibility of using thiols of different lengths as stabilizers for the gold nanoparticles has been reported by Mulvaney and Giersig [6]. This has allowed the facile synthesis of thermally and air-stable gold nanoparticles of reduced dispersity and controlled size. This synthetic technique inspired by Faraday's [7] two-phase system, uses thiol ligands that strongly bind gold due to the soft character of both Au and S [8]. The metal salt is transferred to toluene using the phase-transfer reagent and the reducing agent in the presence of a thiol as shown in Figure 2.1. A two phase method which was originally defined by Wilcoxon *et al.* [9] and later modified by Brust *et al.* [8] formed the basis for the synthesis of metal nanoparticles. These methods produce nearly monodispersed metal nanoparticles particularly in sizes ranging from 2-100 nm.

Other sulfur containing ligands have been used to stabilize gold nanoparticles. Reduction of HAuCl_4 by NaBH_4 in a mixture of tri-*n*-octylphosphine oxide (TOPO) and octadecylamine (ODA) at high temperatures resulted in the controlled growth of spherical AuNPs that were stable for a couple of months [10]. Amino acid lysine capped-AuNPs are stabilized in solution electrostatically, which renders them air-stable and water-dispersible [11]. AuNPs are chemically generated by the reduction of gold precursor by a reducing agent in the presence of a stabilizer which keeps nanoparticles apart, thus avoiding their aggregation. Figure 2.2 shows a scheme for generating AuNPs.

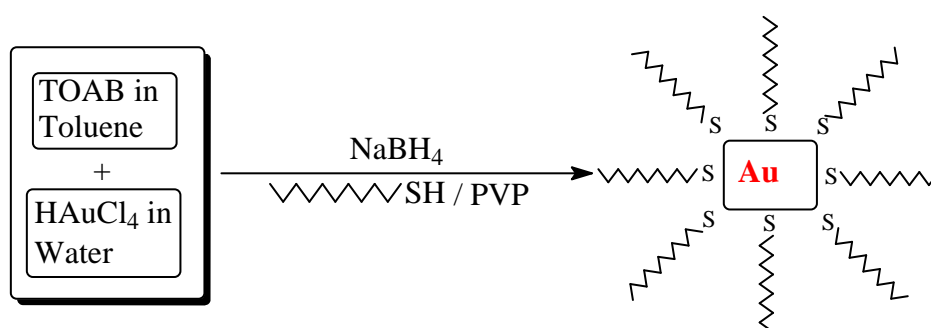


Figure 2.1: Synthesis of AuNPs using Faraday's two-phase technique.

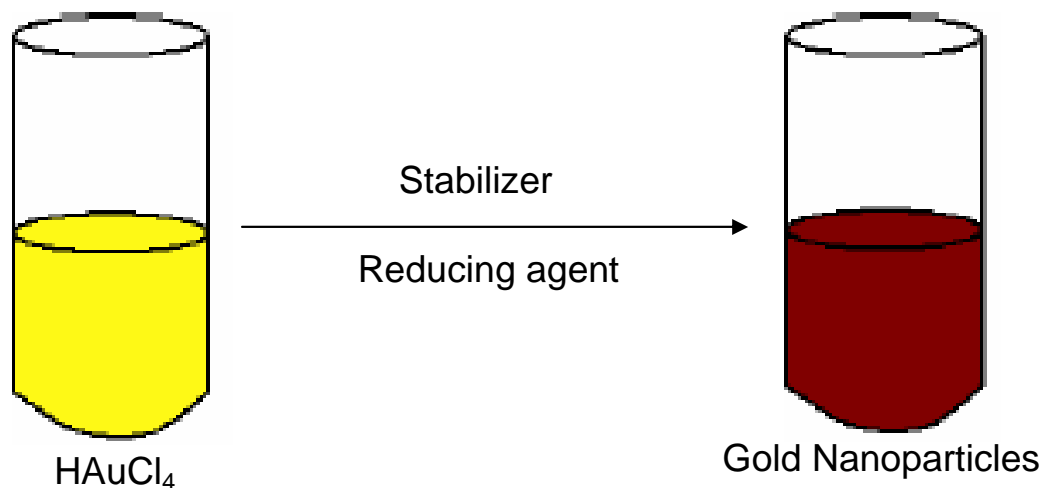


Figure 2.2: Colour changes of gold observed during chemical reduction method.

There are a plethora of techniques for creating nanoscale devices for biomedical engineering and other applications. Many of these, such as chemical reduction techniques, are adaptations of older techniques with more modern and powerful equipment. All of these techniques produce patterns, structures, and surface morphologies at the nanoscale that lead to devices and materials with unique surface properties and functionality. These techniques impart unique chemical, mechanical, electrical, and optical properties to materials for use in electronics, materials science, and medicine.

2.1 EXPERIMENTAL

2.1.1 Materials

The following chemicals were purchased from Sigma-Aldrich and employed during this study without further purification: 1-Dodecanethiol, 4-*tert* butyl pyridine, Acetonitrile, Citric acid, Ethanol, Ethyl glycol, Toluene, Methanol, Glucose, Sucrose, Hydrogen tetrachloroauric acid, Cadmium chloride, Cadmium carbonate, Hydrogen peroxide, Hydrazine monohydrate, L-Ascorbic acid, L-cysteine, Tri-*n*-octylphosphine oxide (TOPO), Octadecylamine (ODA), Hexadecylamine (HDA), Polyethylene glycol (PEG) (10 000 Aldrich), Poly (vinylpyrrolidone) (PVP), Poly (vinyl alcohol) (PVA), Sodium borohydride, Sodium citrate, Sodium hydroxide, Trisodium citrate, Hexadecyltrimethylammonium bromide (HTAB), Tetraethylammonium bromide (TEAB), Tetramethylammonium chloride (TMAC), Tetraoctylammonium bromide (TOAB). High purity double-distilled water was used.

2.1.2 Instrumentation

UV-Vis Optical Spectroscopy

The UV-Vis absorption measurements were conducted using a Perkin Elmer Lambda 20 or Cary 50 Conc. UV-Vis spectrophotometer. The spectra were run by measuring dilute samples in a quartz cell with a path length of 1 cm.

Transmission Electron Microscopy

TEM images were obtained with a Phillips CM120 Biotwin transmission electron microscopy. The specimens were prepared by dropping a dilute solution of the sample containing the nanoparticles on a carbon-coated copper grid and allowing the solvent to dry out at room temperature. The images were captured using the embedded self-imaging system Megaview III digital camera.

X-Ray Powder Diffraction

The wide-angle X-ray diffraction was recorded using the Philips X'Pert Materials Research Diffractometer. Measurements were taken using a glancing angle incidence detector at an angle of 3° for 2θ values over $5 - 100^\circ$ in steps of 0.04° with a count time of 2 s.

2.1.3 Synthesis of Tri-*n*-Octylphosphine Oxide (TOPO) and Octadecylamine (ODA) Capped Gold Nanoparticles

Octadecylamine (ODA, 10.00 g), tri-*n*-octylphosphine oxide (TOPO, 25.00 g) and sodium borohydride (0.0325 g) were mixed together in a three-necked flask under a nitrogen atmosphere. This mixture was heated to 100°C for 1 h, with stirring. After 1 h, the temperature was raised to 190°C . At this temperature, a solution of HAuCl_4 (0.0700 g) dissolved in 4-tert butyl pyridine (5.0 mL) was directly injected into the hot solution, causing a colour change from yellow to red. This solution was maintained at this temperature for 30 min. The reaction mixture was removed from the heating source and cooled to 60°C . Methanol (50.0 mL) was then added, resulting in a precipitation. The precipitation was isolated by centrifugation and rinsed three times with methanol to remove all the by-products, before dispersion in toluene for further analysis. Filtration of the toluene solution yielded an intense red solution of gold nanoparticles, capped with a mixture of TOPO and ODA [12].

2.1.4 Synthesis of Poly-(vinylpyrrolidone) (PVP)-Capped Gold Nanoparticles, using NaBH₄ as a Reducing Agent

PVP (0.400 g) was dissolved in distilled water (25.0 mL) in a beaker under continuous stirring. An aqueous solution of HAuCl₄ (5 mL, 0.0700 g / 0.178 mmol) was then added. A colour change from clear to yellow solution was observed, which clearly indicates the presence of Au³⁺ ions. After 10 minutes of stirring, a freshly prepared NaBH₄ (15.0 µL) was added. A colour change in the solution was observed from yellow to brown. As stirring was continued, a red-wine colour was observed in the solution which confirms the reduction of Au³⁺ ions to Au⁰, the formation of the gold nanoparticles.

2.1.5 Synthesis of PVP-Capped Gold Nanoparticles in the presence of NaOH

HAuCl₄ (0.0700 g) was dissolved in ethanol (20.0 mL) to form a yellow solution containing Au³⁺ ions. In a 100.0 mL round bottom flask PVP (0.400 g) was dissolved in ethanol (50.0 mL) under stirring and nitrogen atmosphere. The two solutions were then mixed in a 100.0 mL round bottom flask to form a light yellow solution. To enhance the reduction of the metal, NaOH (0.10 M; 1.50 mL) was added to form a red-wine solution. The NaOH provides the right pH for reduction to occur. The low yield of nanoparticles was isolated by centrifugation.

2.1.6 Synthesis of PVP-Capped Gold Nanoparticles using Ascorbic Acid as a Reducing Agent

An accurately weighed amount of HAuCl₄ (0.0190 g) and PVP (0.1000 g) were dissolved in distilled water in a 50 mL round bottom flask. The colour of this solution was light yellow and the reaction was performed under nitrogen atmosphere with stirring. Ascorbic acid (0.030 g) was weighed and dissolved in distilled water (10.0 mL). These two solutions were then mixed under constant stirring. Due to the weak ability of ascorbic acid to reduce the metal, the reaction time taken was longer. Initially the colour was observed to be deep yellow (egg yolk), then clear, and finally to light and intense red-wine at maximum reaction time (3 h). This solution was centrifuged and the isolated particles were washed with water. The precipitate was then finally rinsed with ethanol

before further analysis. The concentrations of the reducing and capping agents were further varied to determine their effect on the as-prepared nanomaterials.

2.1.7 Synthesis of PVP-Capped Gold Nanoparticles in the Presence of Sucrose and Glucose

In this typical procedure, gold nanoparticles stabilized by sucrose and glucose were synthesized in separate reactions. In these reactions sodium hydroxide was added in order to initiate the reaction. Typically, PVP (0.300 g), sucrose (0.300 g) and NaOH (0.0200 g) dissolved in distilled water (60.0 mL) in a 100 mL round bottom flask. This solution was then heated in a 60 °C on water bath. To this solution, gold solution (HAuCl₄, 0.0200 g, 10.0 mL), was slowly added drop by drop using a separating funnel. This addition resulted in a colour change forming a wine-red solution. As more gold solution was added the intensity of the colour increased to dark wine-red. The reaction was further left to continue for about 30 min before it was stopped. Particles formed were isolated by centrifugation. Samples at regular intervals for analysis were withdrawn during the reaction. This was done to monitor the growth / formation of the nanoparticles. Another experiment was conducted under similar reaction condition using glucose, instead of sucrose.

2.1.8 Synthesis of PVP-Capped Gold Nanoparticles Using Sodium Citrate as the Reducing Agent

PVP (0.400 g), HAuCl₄ (0.0330 g) and sodium citrate (0.196 g) were dissolved in distilled water (40.0 mL) in a two-necked flask under nitrogen atmosphere, with continuous stirring. The initial colour of this solution was light yellow. This solution was then placed in 100 °C water bath to enhance the metal reduction. During the heating process, as the reaction time increased a colour change to light wine-red and finally to dark wine-red was observed. Heating was stopped and further stirring of the solution was continued overnight. AuNPs were isolated and collected by centrifugation.

2.1.9 Synthesis of PVP-Capped Gold Nanoparticles in Tri-sodium Citrate using NaBH₄ and H₂O₂, as Reducing Agents

HAuCl₄ (0.0330 g), tri-sodium citrate (0.0350 g), PVP (0.1500 g) and H₂O₂ (60.0 μL) were dissolved in distilled water (200.0 mL) under a nitrogen atmosphere. The solution remained light yellow in colour showing the presence of Au³⁺ ions. To enhance the metal reduction, few drops of a freshly prepared NaBH₄ solution (0.50 x 10⁻⁴ M) was added drop-wise and this resulted in a colour change to dark brown indicating the metal reduction. Stirring was continued; a deep wine-red colour was observed in the solution after 1 h. After this reaction time, stirring was discontinued and the solution was centrifuged to isolate the particles.

2.1.10 Synthesis of Dodecanethiol-Capped Gold Nanoparticles Using NaBH₄ as a Reducing Agent

In this procedure dodecanethiol (10.0 mL) was vigorously mixed with 96 % ethanol (60.0 mL) in a 100 mL round bottom flask with continuous stirring. To this mixture, a freshly prepared NaBH₄ (0.50 x 10⁻⁴ M; 2.00 mL) dissolved in ethanol was added. After about 10 min of stirring, HAuCl₄ (1.50 mL, 0.0600 g) dissolved in ethanol was added and stirring was continued for about 30 min. A colour change from a white milky to a creamy solution was observed. As stirring was further continued for two more hours, there was a formation of a colour precipitate which was separated by centrifugation.

2.1.11 Synthesis of PVA-Capped Gold Nanoparticles using Sodium Citrate as a Reducing Agent

PVA (0.400 g) was dissolved in distilled water (40.0 mL) at 80 °C in a two-necked flask. After complete dissolution, the PVA solution was then cooled to room temperature. To this mixture HAuCl₄ (0.0330 g) and sodium citrate (0.1960 g) was added under nitrogen atmosphere with constant stirring. The initial colour of this solution was light yellow. This solution was then placed in 100 °C water bath to enhance the reaction. During the heating process a colour change from light yellow to light wine-red and finally to dark wine-red was observed. The heating was discontinued, but further stirring

of the solution was continued overnight. The resultant particles were isolated by centrifugation.

2.2 RESULTS AND DISCUSSION

2.2.1 Synthesis of TOPO-ODA Gold Nanoparticles

O'Brien and Green have reported the reduction of HAuCl_4 by NaBH_4 in a mixture of TOPO and ODA (1:0.57 molar ratio) at 190 °C [10]. Under these conditions spherical and stable nanoparticles in toluene were obtained, which were also manipulated into crystals and 3D arrays. Selvakannan *et al.* [13] reported the one-step synthesis of organically dispersible spherical AuNPs using the multifunctional molecule hexadecylamine (HDA). They showed that aqueous chloroaurate ions might be phase-transferred into chloroform by electrostatic complexation with HDA molecules present in the organic phase. Since they both (HDA and ODA) carry an amine functional group, similar behavior in their nanoparticles is expected. Other synthetic methods of this nature were reported by Murray and co-workers [14] for the synthesis of (II/VI) or (III/V) semiconductor quantum dots capped with TOPO. Green and co-workers [15] reported the synthesis of trialkyl phosphine oxide/amine stabilized silver nanocrystals. Recently Nath *et al.* [16] have reported the synthesis of HDA-capped silver organosols which were stable for over a year. Chen *et al.* [17] developed a very important method for synthesizing monodispersed silver nanoparticles where tri-octylphosphine (TOP) was used as the reducing agent, solvent and surfactant.

Figure 2.3 shows the UV-Visible spectrum of TOPO and ODA capped gold nanoparticles. In this method TOPO, ODA and NaBH_4 were all heated to 100 °C. At this temperature, HAuCl_4 in 4-*tert*-butyl pyridine was directly injected, resulting in TOPO-ODA-capped AuNPs. When particles of gold are small enough, their colour is ruby red, due to their strong absorption of green light at about 520 nm, corresponding to the frequency at which a plasmon resonance occurs with the gold. The appearance of this light absorption of metallic nanoparticles is due to the oscillation of the conduction electrons induced by interacting electromagnetic field and this resonance is called surface plasmon resonance (SPR), the resonance can be influenced by size, shape and dielectric

constant of the medium in which the nanoparticles were dissolved [18]. This dominant visible absorption spectrum related to metal nanoparticles originated from group 11 is believed to originate from the surface plasmon resonance. This SPR phenomenon has been extensively studied in other related papers and can be predicted by Mie theory [19,20,21]. The particle shape depends on the reaction conditions such as concentration of reagents, reaction temperature and time. A combination of these reaction parameters can result in a variety of particle shapes. El-Sayed *et al.* [22] and Murphy *et al.* [23] have shown that nanorods of gold exhibit two SPR peaks, with the wavelength of transverse mode located at 525 nm and the wavelength of longitudinal mode tunable in the spectral region from visible to near-infrared depending on their aspect ratios.

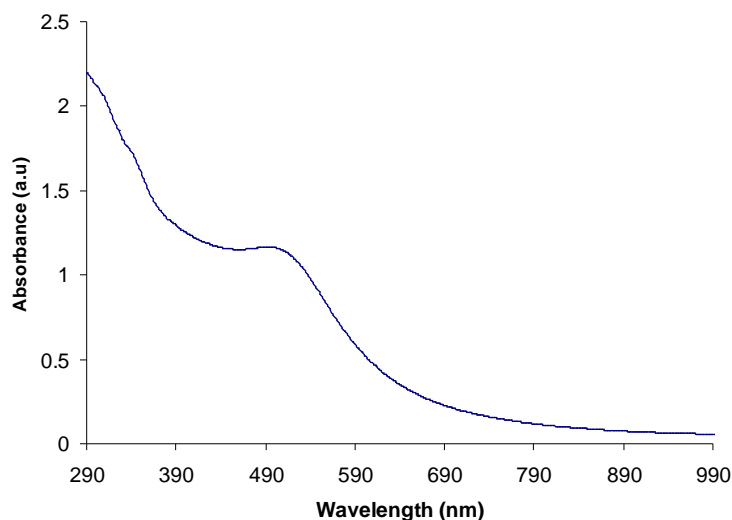


Figure 2.3: UV-Visible spectrum of TOPO-ODA-capped gold nanoparticles.

As the aspect ratio of the rods increase the major longitudinal band shifts to the red. When the particle shape changes to triangular plates or polygonal, the SPR band appears in the 550 - 700 nm regions. As shown in Figure 2.4, these nanoparticles provide a platform to tune the SPR band in the spectral range from 400 – 750 nm. Bulk gold has a familiar yellow colour, caused by the reduction in reflectivity for light at the end of the spectrum [24]. Figure 2.5A, shows the transmission electron microscopy (TEM) image of TOPO-ODA-capped gold nanoparticles. Most of the gold nanoparticles were spherical in shape. The average size of the nanoparticles produced is 7.29 ± 1.01 nm, as seen on the

size distribution graph [Figure 2.5B]. The TEM image shows that the solution contains predominantly spherical nanoparticles which are well dispersed on the grid, with particles in the shape of triangles also observed. The single absorption peak observed in the UV-Visible absorption spectrum analysis confirms the predominance of spherical particles.

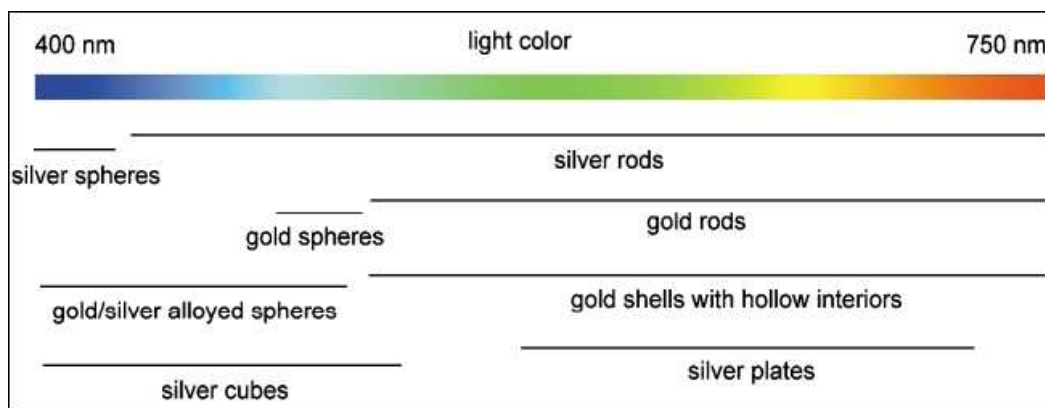


Figure 2.4: A list of silver and gold nanoparticles having various morphologies, compositions, and structures, together with their typical locations of SPR bands in the visible regime [25].

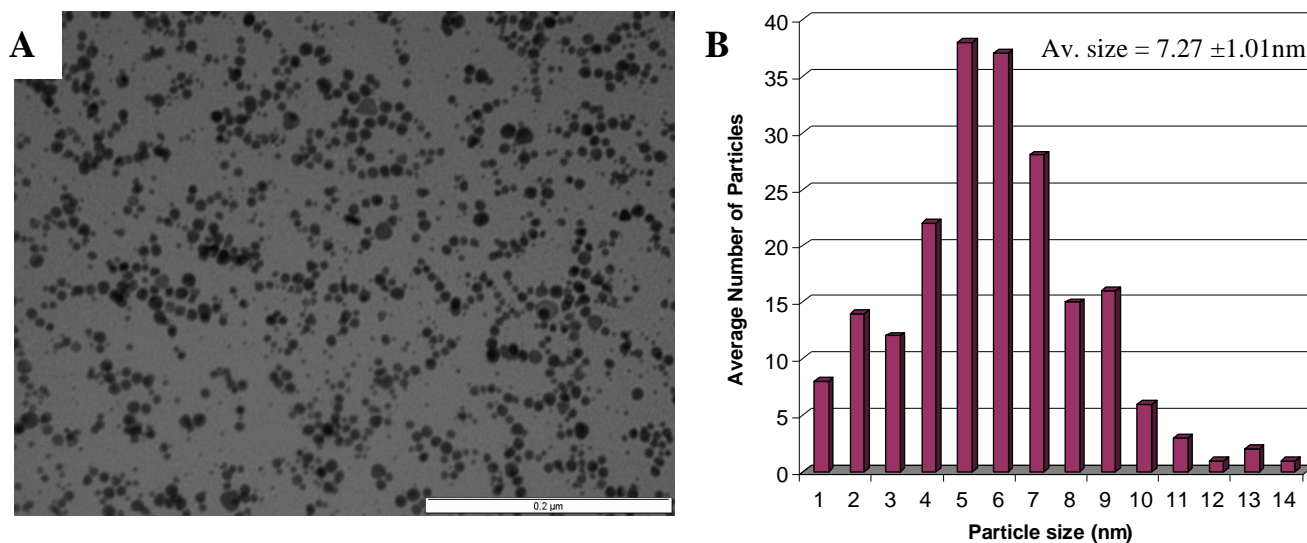


Figure 2.5: A) TEM image and B) Size distribution graph of TOPO-ODA-capped AuNPs.

2.2.2 Synthesis of PVP-Capped Gold Nanoparticles

The synthesis of gold nanoparticles by the reduction of Au^{3+} ions in the presence of PVP and PVA as stabilizers is reported. NaBH_4 , NaOH and ascorbic acid were used as reducing agents. Basically in this synthetic method, a capping polymer and HAuCl_4 were dissolved in the respective solvents followed by the addition of a reducing agent. Figure 2.6 shows the UV-Visible spectrum of PVP-capped gold nanoparticles reduced by both NaOH and NaBH_4 respectively. The light yellow colour of the aqueous HAuCl_4 solution changes to brown, then to wine-red at longer reaction time. The colour change to wine-red was also confirmed with the appearance of a peak at 520 nm due to the SPR absorption of spherical gold nanoparticles [26,27]. The formation of the brown colour was noticed after the immediate addition of NaBH_4 . A gradual change to wine-red with the increase in reaction time was then observed. The UV-Visible spectra of the PVP capped particles synthesized with the assistance of NaOH are shown in Figure 2.6A. The spectrum exhibits a sharp, single absorption at 530 nm which corresponds to the known surface plasmon absorption band of gold nanoparticles. Sodium hydroxide was introduced into the system just to stabilize the nanoparticles and also to speed the reduction of the metal without using any known reducing agent in ethanol. This single absorption peak indicates the presence of mostly small and spherical nanoparticles.

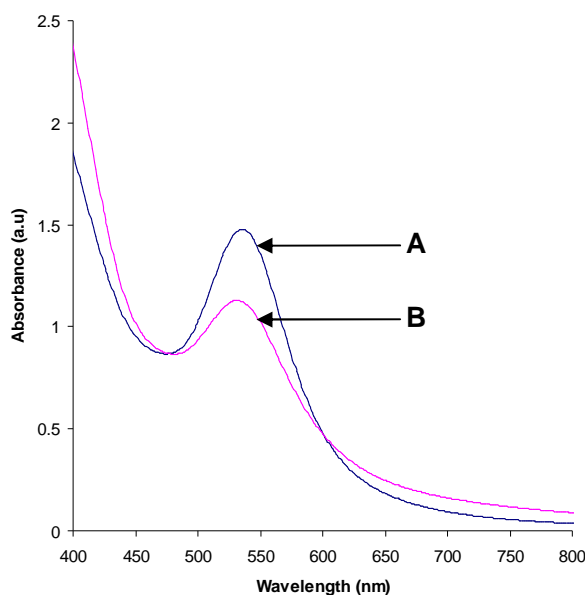


Figure 2.6: UV-Visible spectrum of PVP-capped gold nanoparticles in the presence of A) NaOH and B) NaBH_4 .

Figure 2.7 shows the transmission electron microscopy (TEM) images of gold nanoparticles prepared from the above method. Figure 2.7A shows nanoparticles capped by PVP and reduced with NaBH_4 to have its average size of the particle to be within the range of 20 – 40 nm. The gold particles formed with the assistance of NaOH are shown in Figure 2.7B. A wide range distribution of nanoparticles is observed from different parts of the copper grid with the spherical particles dominating in the yield. The image show nanoparticles within 10 - 20 nm in size range. Both samples aggregated spherical nanoparticles.

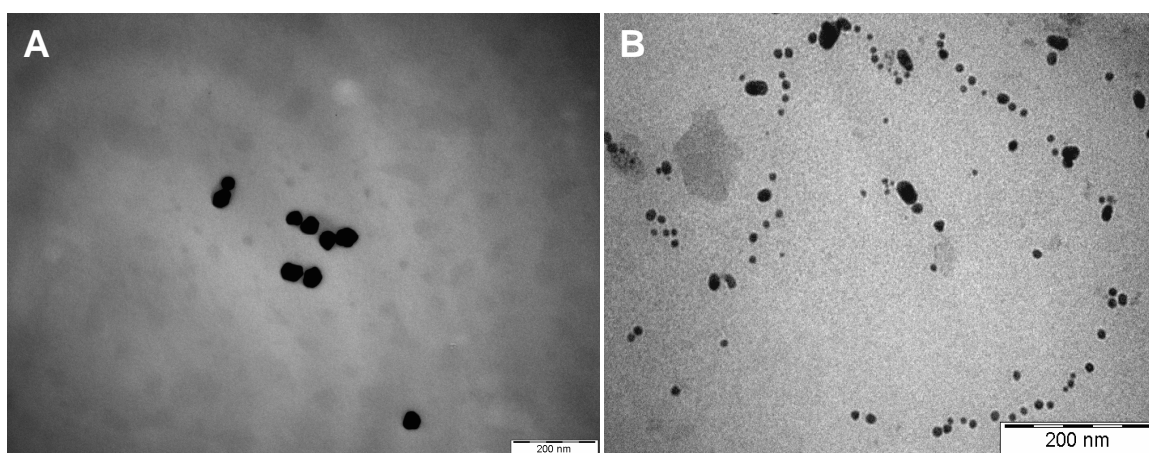


Figure 2.7: TEM images of PVP-capped gold nanoparticles in the presence of A) NaBH_4 and B) NaOH.

UV-Visible spectroscopy and TEM were used to determine the optical and structural properties of the PVP-capped gold nanoparticles using ascorbic acid as the reducing agent. Figure 2.8 displays typical spectra indicating the absorption around 538 nm for different concentrations of the reducing agent; A (0.03 g); B (0.06 g); C (0.075 g). The absorption at low concentration of ascorbic acid (0.03 g) shows a clear and sharp peak. Higher concentrations (B and C) show a red shift and broad yet informative peak exhibiting clear absorption corresponding to surface plasmon resonance of gold nanoparticles with few distinct features. The plausible explanation of the broad spectrum observed at these concentrations is that it could possibly originate from the presence of non-spherical nanoparticles with a wide distribution of particle sizes. The exact mechanism for the formation of different shape and morphology of gold nanoparticles is

still unclear. However, EI-Sayed *et al.* [28] provided two reasonable explanations for the formation of faceted particles: (i) the growth rates vary at different planes of the particles, (ii) particle growth competes with the coordinating action of stabilizers. During the course of the preparation of nanoparticles, polymers are often used which selectively adsorb on certain crystal planes and induce anisotropic growth of different planes.

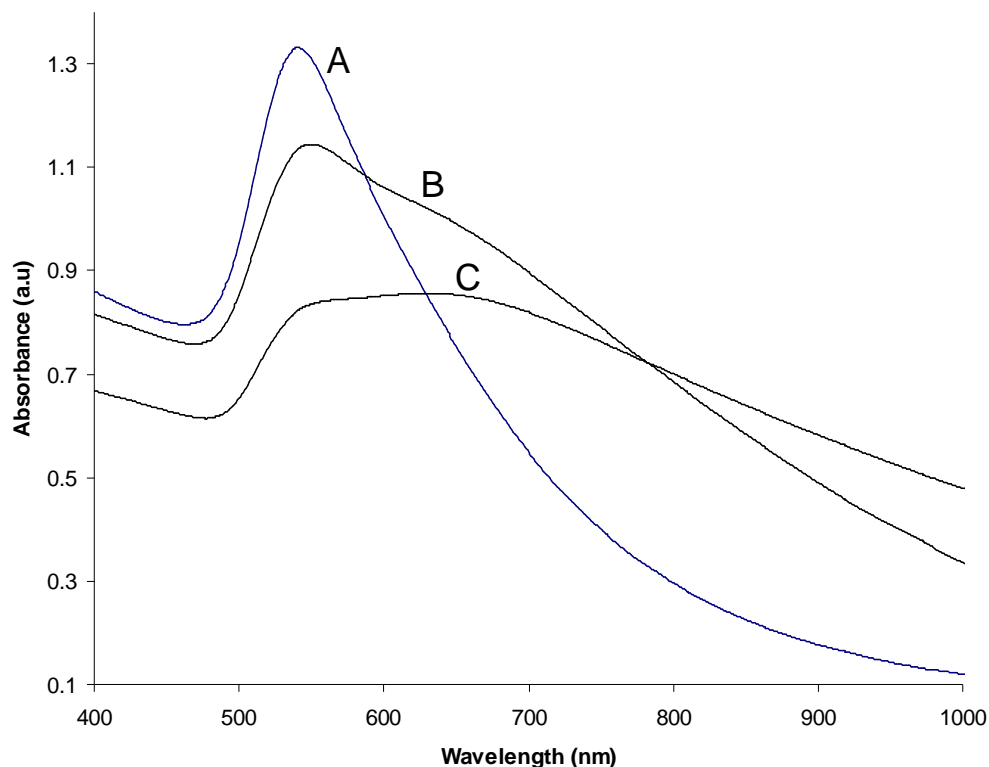


Figure 2.8: UV-Visible spectra of gold nanoparticles at different concentrations of the reducing agent; A. (0.03 g); B. (0.06 g); C. (0.075 g) in ascorbic acid.

Figure 2.9 shows the absorption spectra of gold nanoparticles synthesized by varying the concentration of the stabilizing agent. Except for peak intensity, the spectrum shows no distinct differences in the absorption wavelength due to the change of the polymer concentration. These absorption results are summarized in Table 2.1 for the variation of the reducing and stabilizing agents. Figure 2.10 shows the transmission electron microscopy (TEM) analysis for the gold nanoparticles prepared with a low concentration of ascorbic acid (0.03 g). The micrograph shows large nanoparticles which are aggregated. Figure 2.11 and 2.12 shows the TEM images of gold nanoparticles which

were synthesized by varying the concentration of the stabilizing agent. The images presented in Figure 2.11 were samples of a lower concentration of the polymer (0.02 g) and at different magnifications as well as in random parts of the copper grid.

Table 2.1: Absorption maxima of gold nanoparticles at different concentrations of the capping and reducing agents.

H ₂ AuCl ₄ (g)	PVP (g)	Ascorbic acid (g)	Absorption maximum (nm)
0.019	0.100	0.030	538
0.019	0.100	0.060	546
0.019	0.100	0.075	540 - 700
0.019	0.020	0.022	534
0.019	0.040	0.022	534

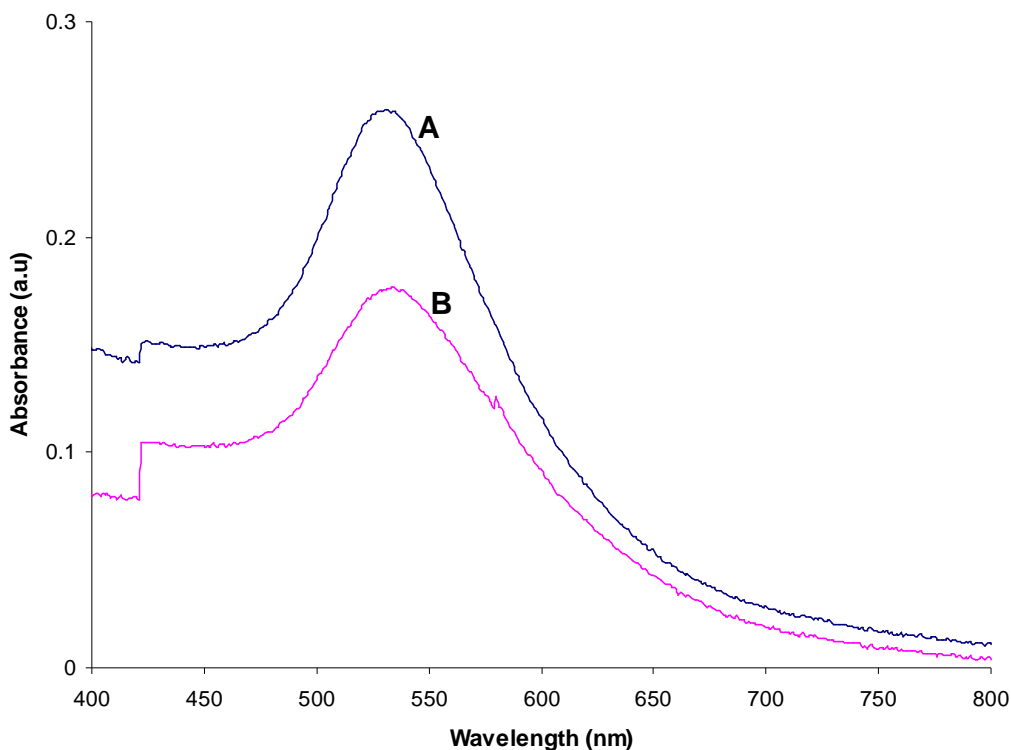


Figure 2.9: UV-Visible spectra of PVP-capped AuNPs at different concentrations of the capping agent; A. (0.02 g); B. (0.04 g) reduced with ascorbic acid.

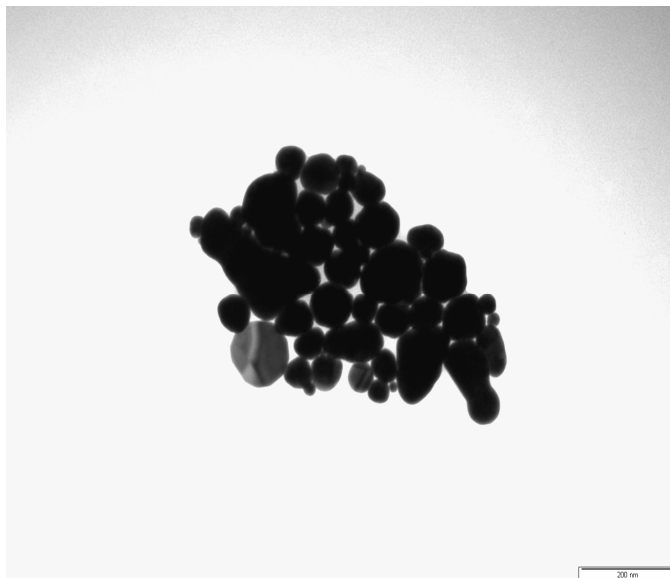


Figure 2.10: TEM micrograph of PVP-capped gold nanoparticles at low concentration of ascorbic acid (0.03 g).

These TEM images consist of rounded, star polyhedral gold nanocrystals, multiple-twinned with five-fold symmetry and more nanoparticles with indefinite shapes as indicated in the high magnification image in [Figure 2.11C](#). Most of these nanoparticles are approximately 50 nm in size. [Figure 2.11D](#) shows an elongated, spherical, short but broad rod and hexagonal shaped nanoparticles. As the ratio of capping to reducing agent was increased, many star-shaped gold nanoparticles were observed as shown in [Figure 2.12](#). These star polyhedral gold nanoparticles produced are in agreement with those synthesized by Burt *et al.* [29] who concluded that the reducing agent played a crucial role in the production of these star gold nanocrystals. Well defined triangular and hexagonal shape nanoparticles are observed in high magnification images shown in [Figure 2.12C](#) and [D](#). The crystal phase of the particles was determined by the X-ray diffraction technique. [Figure 2.13](#) shows the X-ray diffraction pattern of gold nanoparticles reduced by ascorbic acid at low concentration of stabilizer with the (111), (200), (220) and (311) planes of gold are clearly observed. These peaks demonstrate that the as-prepared products are of purely crystalline gold with a face-centered cubic structure (JCPDS File 04-0784).

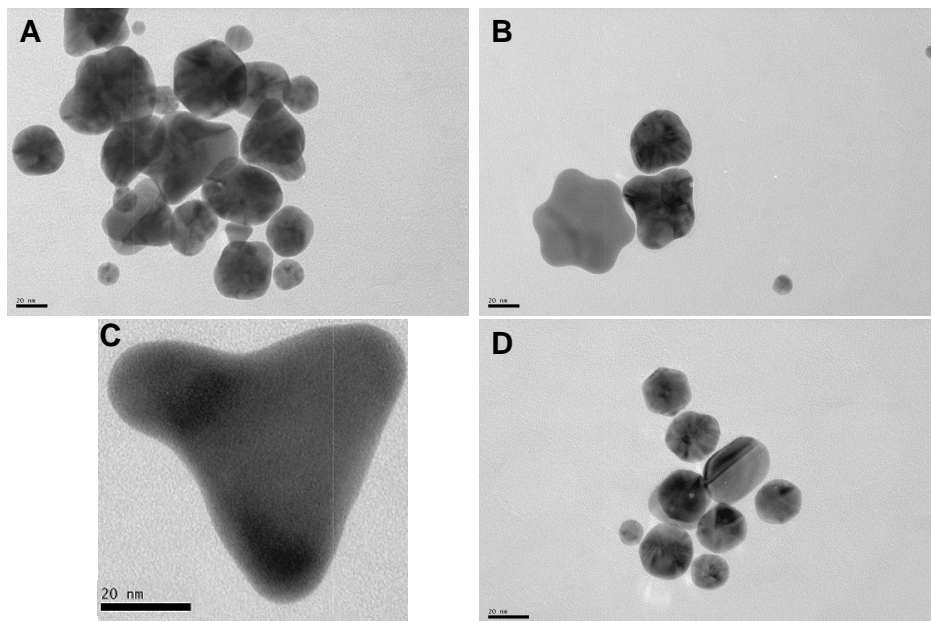


Figure 2.11: A, B and D are TEM micrographs of AuNPs at low concentration of capping agent (0.02 g) reduced by ascorbic acid taken from different parts of the Cu grid; C is the high resolution TEM micrograph.

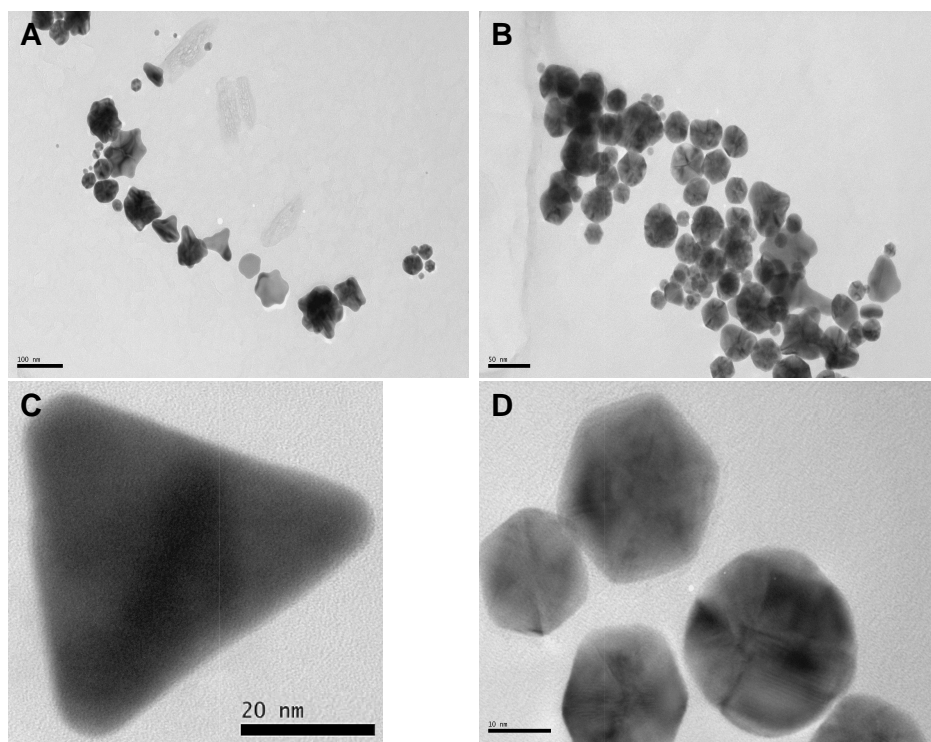


Figure 2.12: A and B are TEM micrographs of AuNPs at high concentration (0.04 g) of capping agent reduced by ascorbic acid taken from different parts of the Cu grid; C and D are the high resolution TEM micrographs.

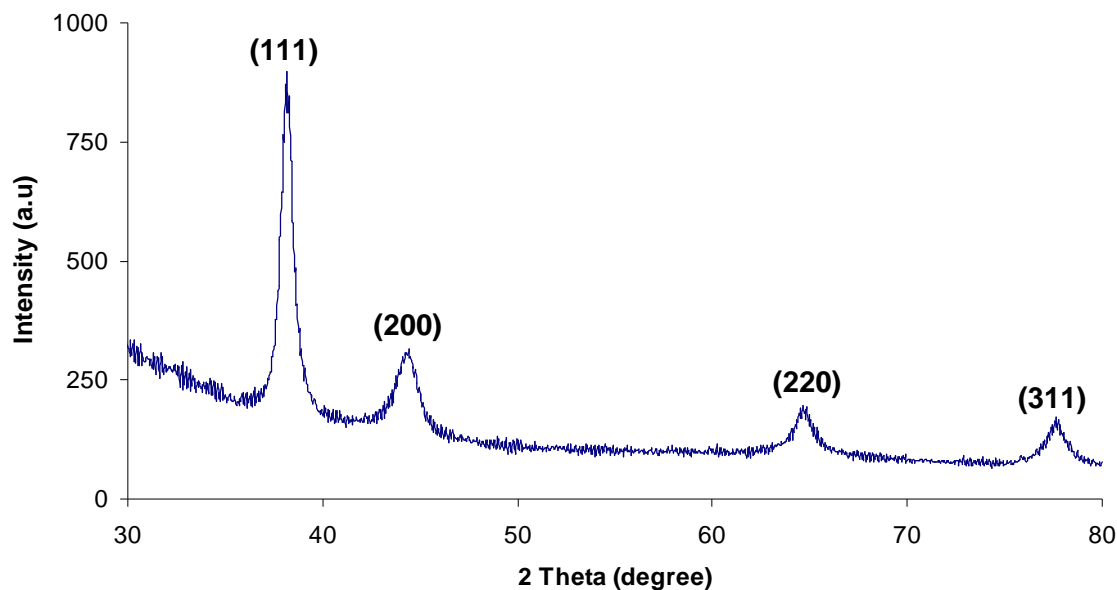


Figure 2.13: XRD pattern of PVP-capped Gold Nanoparticles reduced by ascorbic acid at low concentration of stabilizer (0.02 g).

PVP-capped gold nanoparticles were synthesized in the presence of sucrose and glucose. In this particular synthetic procedure, AuNPs were formed by dissolving PVP, one of the sugars and a small amount NaOH in order to enhance the reaction. This solution was warmed and finally HAuCl_4 solution was added drop-wise as described in section 2.1.7. Figure 2.14 shows the UV-Visible spectra of such metal nanoparticles in the sucrose and glucose. They both show characteristic SPR absorption maximum at around 535 nm, which is an indication of the formation of gold nanoparticles. In both the experiments the growth was monitored by removing solutions for optical analysis before completely adding the gold solution. There was not much of a difference observed in the absorption wavelength except a reduction in intensity at shorter reaction time. The UV-spectra reported for both the nanoparticles in sucrose and glucose were taken at the longest time of the reaction, i.e. 30 minutes. Figure 2.15 shows the TEM micrographs for the synthesized nanomaterials. The particles synthesized in both sugars were predominantly spherical in shape with sizes ranging from 5 - 15 nm.

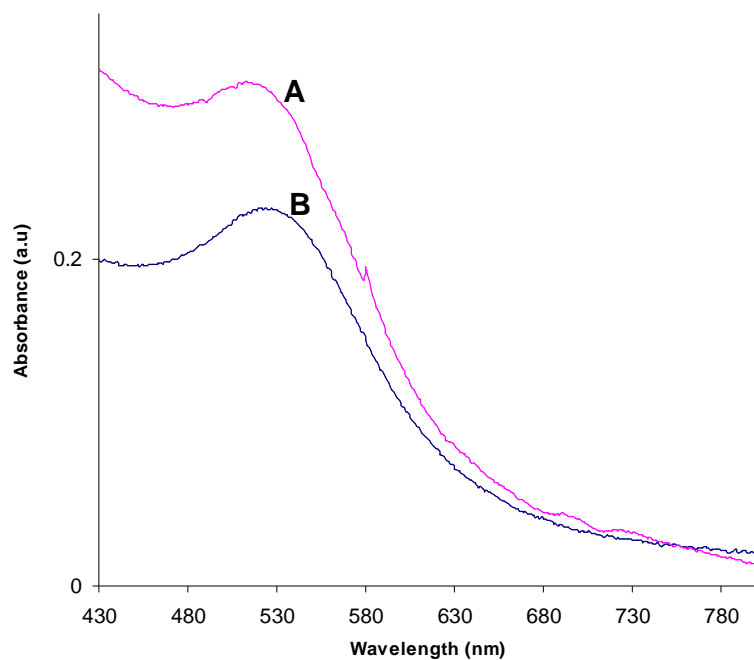


Figure 2.14: UV-Visible spectra of PVP-capped AuNPs in A) glucose and B) sucrose.

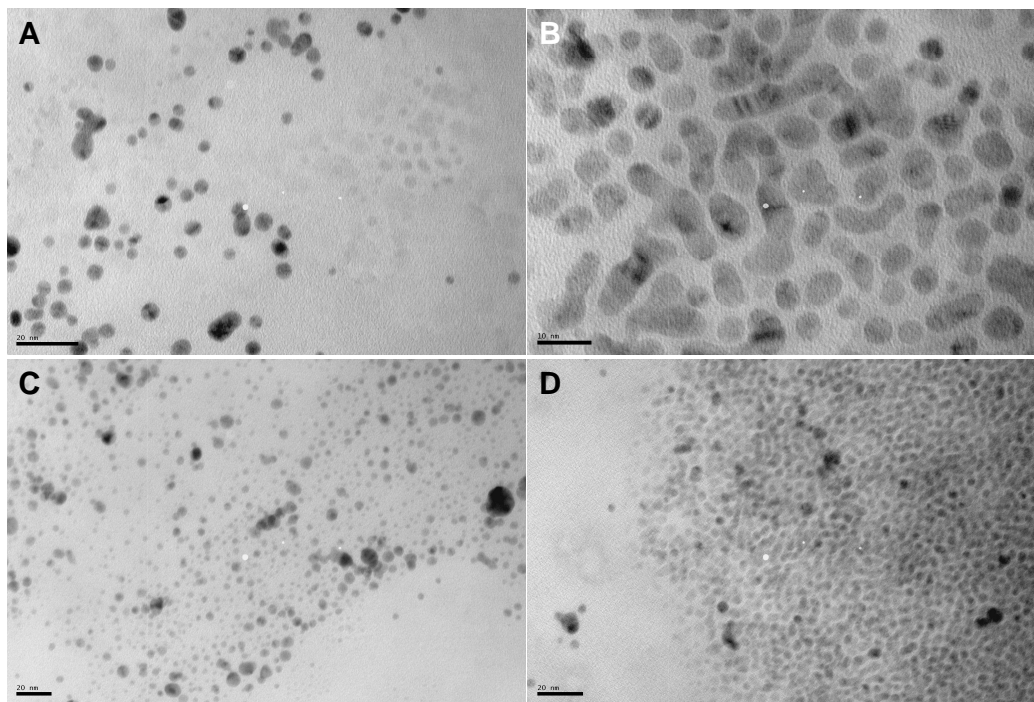


Figure 2.15: TEM micrographs of PVP-capped gold nanoparticles in [A. and B. (sucrose)], [C. and D. (glucose)].

The analysis of gold nanoparticles which were synthesized by the reduction of Au^{3+} ions, in the presence of heat, using sodium citrate and NaBH_4 as reducing agents is reported. Figure 2.16 shows the UV-Visible spectra of the solution mixtures of the three distinct reactions performed. Basically in these methods, a capping agent, HAuCl_4 and sodium citrate were all dissolved in water and heated to $100\text{ }^\circ\text{C}$ in order to enhance the reaction. In the reaction where NaBH_4 was used as the reducing agent, a small amount of hydrogen peroxide, (H_2O_2) was added. The light yellowish colour of the aqueous HAuCl_4 solution exhibits an intense band at 292 nm because of a metal-ligand charge transfer band from the AuCl_4^- complex [14]. As the reaction progresses, the colour change to wine-red with the appearance of new peaks between 520 nm and 530 nm due to the SPR absorption.

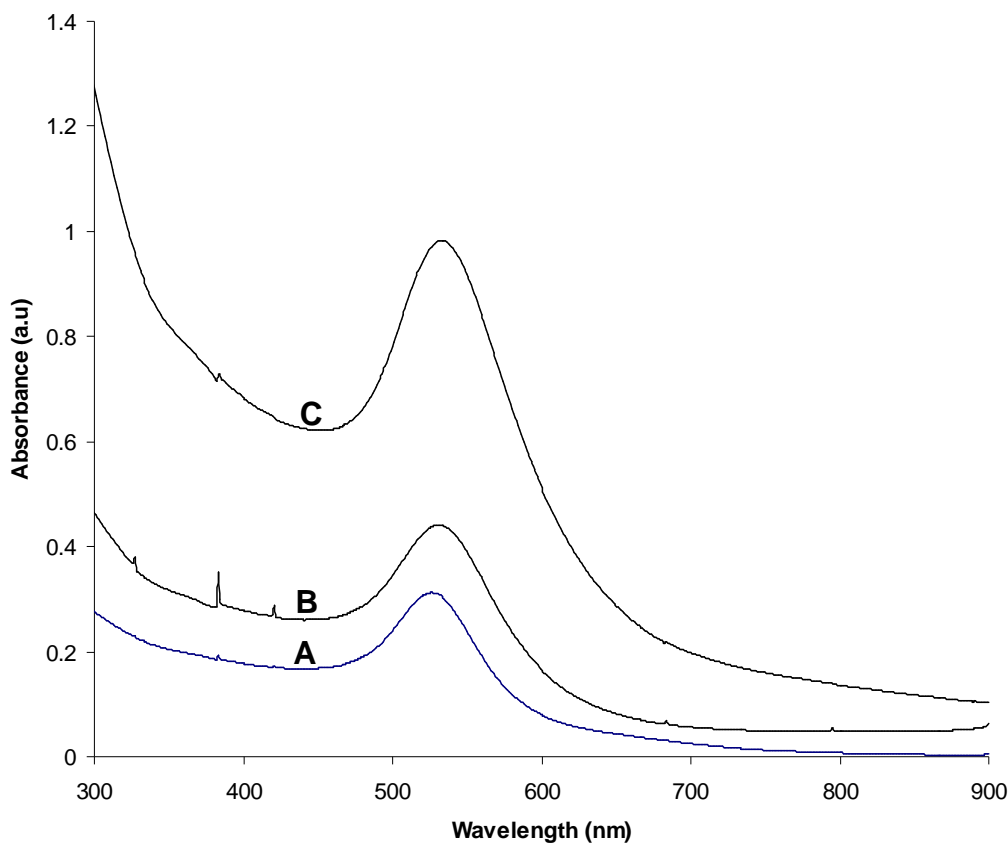


Figure 2.16: UV-Visible spectra of gold nanoparticles: A) [PVP and heat], B) [PVA and heat] and C) [NaBH_4] in sodium citrate.

Figures 2.16 A and B are the absorption spectra of gold nanoparticles where heat was used to enhance the reaction in the presence of PVP and PVA as stabilizing agents respectively. Their corresponding absorptions are 522 nm and 528 nm, which is within the gold nanoparticle absorption region. In these two reactions the formation of wine-red colour observed after few seconds of exposure to heat and the colour intensity increased gradually with heating and became saturated after about 4 min indicating the completion of the reaction. Figure 2.16 C shows the absorption of gold nanoparticles at 530 nm prepared with the assistance of NaBH_4 where PVP was used as a stabilizing agent. The absorption is red-shifted in relation to the particles synthesized in the presence of heat. This shift is probably due to the presence of anisotropic particles.

Figure 2.17 shows the TEM images of gold nanoparticles prepared by the reduction of Au^{3+} ions with sodium citrate in the presence of PVP as the stabilizing agent. The image shows the presence of anisotropic particles in the shape of triangles, rods, pentagons and hexagons. At high magnification the nanoparticles with lattice planes are observed as shown in Figure 2.17 A and B, with size ranging from 10 - 40 nm. The gold nanoparticles stabilized with PVA did not show much shape variation as observed in the PVP stabilized particles. Figure 2.18 A shows predominantly spherically shaped gold nanoparticles with a small percentage of anisotropically shaped nanoparticles. The particle size is within the 30 - 40 nm range. Figure 2.18 B shows the micrograph of gold nanoparticles prepared by the assistance of NaBH_4 as the reducing agent in PVP and H_2O_2 . In this image monodispersed, spherical nanoparticles are observed. The obtained nanoparticles are slightly larger with an average particle size of 46.4 ± 9.25 nm. Figure 2.19 shows the results obtained from the X-ray powder diffraction (XRD) pattern for the PVP and PVA stabilized gold nanoparticles. The peaks at $2\theta = 38.2^\circ$; 44.5° ; 64.9° and 77.9° correspond respectively to the (111), (200), (220) and (311) planes of gold. These peaks demonstrate that the as-prepared products are of purely crystalline gold with face-centered cubic structure (JCPDS File 04-0784).

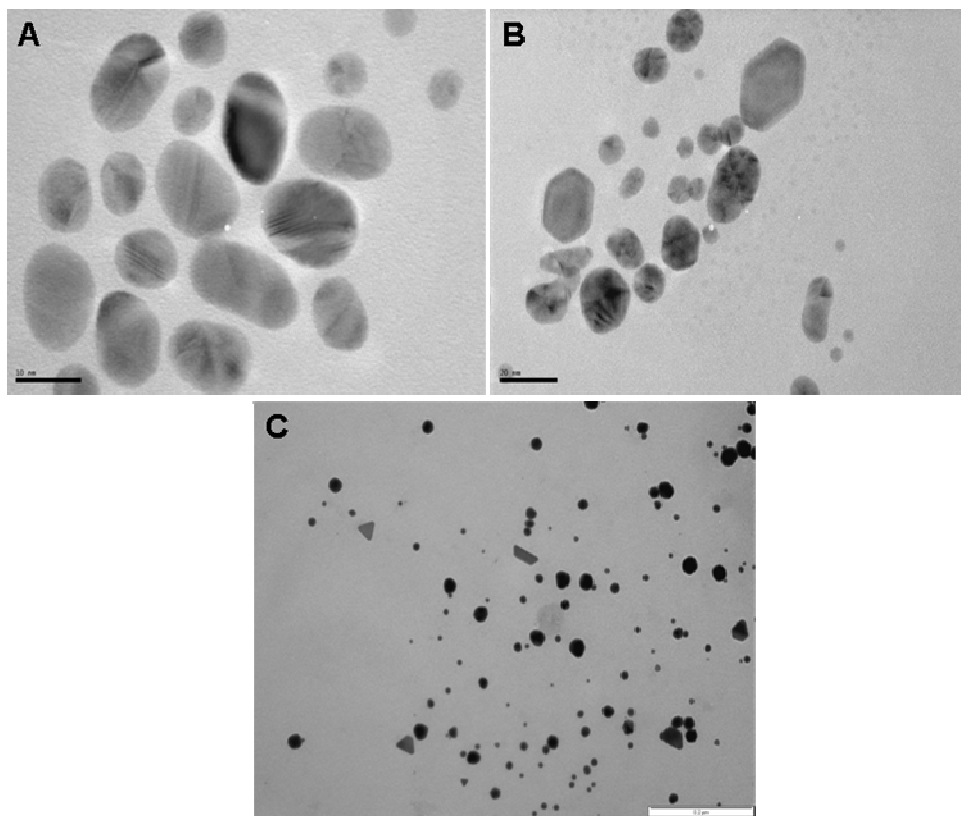


Figure 2.17: A, B and C are TEM micrographs of PVP-capped gold nanoparticles from different parts of the Cu grid reduced with sodium citrate.

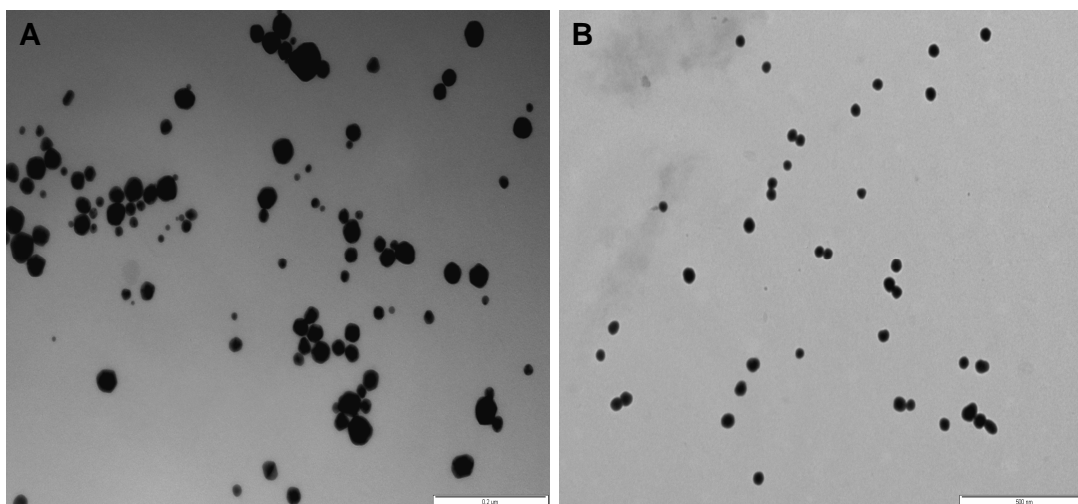


Figure 2.18: TEM micrographs of gold nanoparticles; A) PVA-capped reduced with sodium citrate and B) PVP-capped in NaBH_4 and sodium citrate.

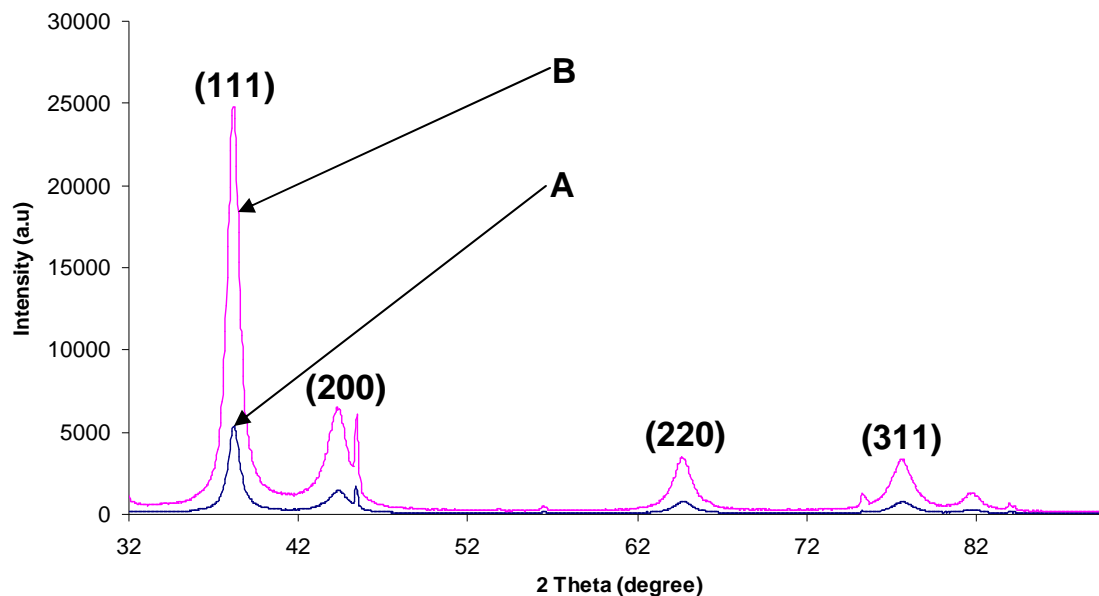


Figure 2.19: XRD pattern of gold nanoparticles stabilized by A) PVP and B) PVA; all reduced with sodium citrate.

2.2.3 The Role of Poly vinyl Pyrrolidone (PVP)

The shape and the size of gold nanowires depend upon the adsorption of PVP on the surface of the gold particles [30]. Previous studies have also found that increasing the chain length of PVP resulted in a change of shape for gold and silver nanostructures from 2D plane structures to 1D rod and wire structures [30]. PVP plays an important role in controlling the growth rate between the $\{100\}$ and $\{111\}$ plane directions [31]. Reyes-Gasga *et al.* proposed that nanowires evolve from a multiply twinned nanoparticle (MTP) of silver with the help of PVP at the initial Ostwald ripening stage [32]. The growth of the nanowires was facilitated by PVP selectively covering the $\{100\}$ facet. This is done through chemical interactions with the nitrogen and or oxygen atoms of the pyrrolidone units of PVP [33]. On the other hand the interaction between PVP and the $\{111\}$ facet is weaker allowing the nanowires to grow continuously during the Ostwald ripening process. Due to force fields which exist between atoms, they will begin to agglomerate to form colloidal gold particles which are dominated by the $\{110\}$ facet. The $\{110\}$ facet forms a weak interaction with the PVP molecules due to the weak binding energy. Gold nanoparticles with larger sizes will be able to grow at the expense of smaller one through agglomeration and Ostwald ripening. As growth continues the polygonal particles begin

to form which have both {100} and {111} facets. In the literature it is reported that PVP could bind stronger with the {100} plane as compared to the {111} plane [34]. Since there is a competition between {111} and {100} facets to absorb PVP molecules, a certain amount of PVP will be adsorbed on each facet. In this case the {100} facets will absorb more PVP molecules. In the case where a certain amount of PVP is absorbed on the {111} facets, the polygonal particles will appear in solution as growth will occur on the {100} facets.

In comparison, the interaction between PVP and the {111} facets should be much weaker to enable the two ends of the nanorods to grow continuously throughout Ostwald ripening. Concentration of PVP does not favour the formation of pentagonal and trigonal shaped particles. The high concentration of PVP leads to the formation of a thick coating over the entire surface of the spherical particles, including the twin boundaries [35]. Therefore selective interaction between PVP and various crystallographic planes are lost and thus no anisotropic growth could be induced. The reaction temperature also plays a significant role in controlling the morphology of gold nanoparticles.

2.2.4 Synthesis of Dodecanethiol-Capped Gold Nanoparticles

Decahedron and icosahedron of alkanethiol-capped gold nanoparticles were first observed by Mihama *et al.* [36] who analyzed and characterized these particles as “multiple twinned particles” (MTPs). Du *et al.* [37] also prepared gold nanoparticles using this method. Decahedron shaped particles obtained in their experiments displayed different absorption behavior compared to conventional gold colloid. In their experiment they also found that the molar ratio of *n*-dodecanethiol to H₂AuCl₄ played a key role in forming decahedrons of gold nanoparticles which was consistent with the results obtained by Kimura *et al.* [38]. The optical and structural properties of the dodecanethiol-capped gold nanoparticles are reported in this work. The alkanethiol-capped gold nanoparticles were synthesized by the reduction of H₂AuCl₄ with NaBH₄ in ethanol. These nanoparticles display an absorption shoulder in the 350-370 nm region with a broad SPR absorption maximum at 520 nm as shown in [Figure 2.20](#).

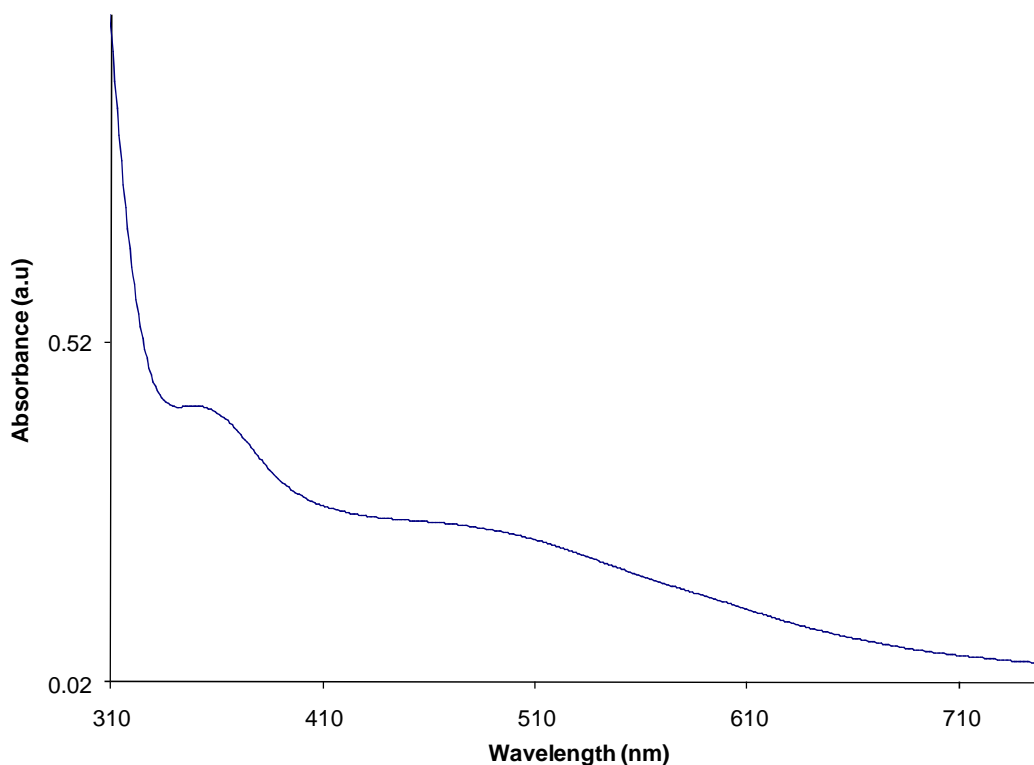


Figure 2.20: UV-Visible spectrum of dodecanethiol-capped gold nanoparticles.

The broadened absorption peak could be due to large anisotropic particles with a broad size distribution. The deviation from spherical geometry is also explained by Mie's theory, suggesting in the circumstance that the transverse and longitudinal dipole polarizability no longer produces equivalent resonance, leading to a broadening and red shift of the longitudinal plasmon resonance as well as an appearance of transverse plasma resonance. [Figure 2.21A](#) and [B](#) shows dodecanethiol-capped nanoparticles TEM images at different magnifications. The image reveals particles in the shape of rods, pentagons, hexagons and truncated triangles. In the pentagonal nanoparticles the five-fold twinned crystal structure on their topology which was also observed in the case of Ag by Xia *et al.* [39].

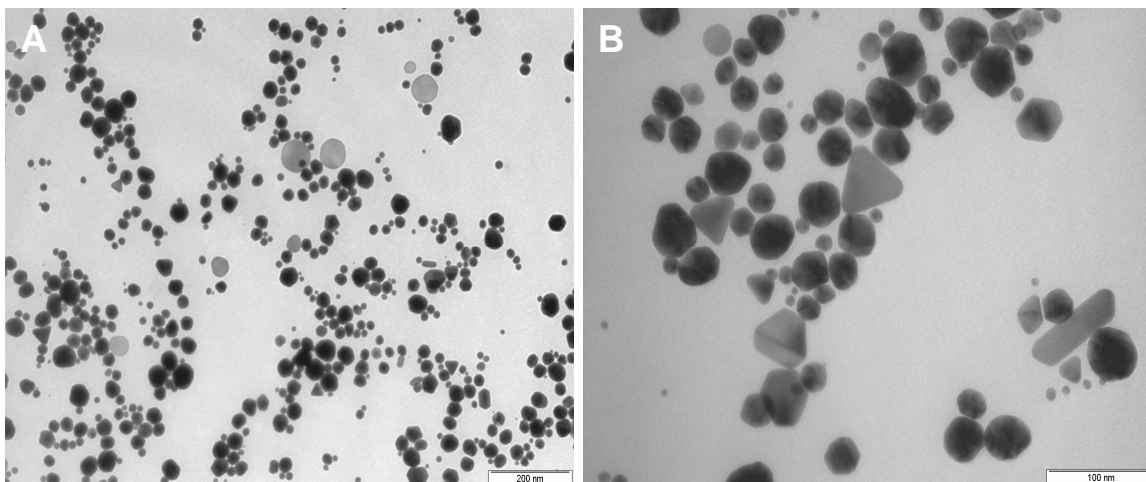


Figure 2.21: *A and B are TEM micrographs of dodecanethiol-capped gold nanoparticles at different magnification.*

This anisotropic formation of gold nanoparticles also confirms the broadening observed at the UV-Visible spectrum. Dodecanethiol plays a similar role to PVP in the formation of anisotropic gold nanoparticles.

2.3 SEED-MEDIATED AND PHASE-TRANSFER SYNTHESIS OF GOLD NANOPARTICLES

2.3.1 Introduction

Non-spherical gold nanoparticles have gathered significant attention due to their intriguing shape-dependent properties, including multi-modal plasmon resonance and fluorescence, which make them promising candidates as tagging agents and surface enhanced Raman scattering substrates, amongst other applications. Synthesis of shaped nanoparticles such as rods [40], prisms [41], hexagonal plates [42], cubes [43] and stars [44] have been reported. The most common route to shaped nanoparticles is through seeded-growth methods. A chemical reducing agent is used, where small, generally spherical nanoparticles are first generated and then added to a growth solution with more metal ions and surfactant to induce anisotropic growth. The slight changes in reactant ratio, use of different seeds, variations in pH and stabilizer concentrations are adjusted to

control the morphology of the nanoparticles. Counter ions and additives have also been found to play a role in directing the growth and the final shape of nanoparticles obtained.

In seeded growth reactions, a previously synthesized "seed" nanoparticle is introduced to a growth solution containing a Au(III) salt, a weak reducing agent, and a directing agent (most commonly a surfactant). Initially, the seed particles grow through the slow-diffusion of gold atoms onto their surface. Currently, shape-controlled synthesis of nanoparticles has been achieved either by using geometric templates [45], or by using some additives [46], such as polymers or inorganic anions [47], to regulate the particle growth. Natan *et al.* proposed a seed-mediated approach to grow preformed, spherical gold nanoparticles in solution, based on the gold colloid surface catalyzed reduction of Au³⁺ by hydroxylamine [48]. Alternatively, seeds could be grown using sodium citrate as a reductant, producing Au nanoparticles with dimensions between 20 and 100 nm of improved monodispersity relative to the original Frens method [49]. These authors have pointed out that iterative hydroxylamine seeding leads to the formation of a distinct of colloidal gold rods.

Jana *et al.* studied the growth of citrate stabilized gold nanoparticles by the seed-mediated method using a wide range of reducing agents and conditions [50]. They showed that even in the presence of seeds, additional nucleation takes place. Additional nucleation can be avoided by controlling critical parameters such as the rate of addition of reducing agent to the metal seed and metal salt solution and the chemical reduction potential of the reducing agent. A step-by-step particle enlargement method also allows a large seed to metal salt ratio to be maintained throughout successive growth steps. Using this approach, Murphy *et al.* were able to prepare spherical particles in a size range 5 – 40 nm with relatively uniform size [51]. The primary nuclei were 3.5 nm gold seeds prepared by borohydride reduction of gold salt in the presence of citrate as capping agent. The growth steps were carried out in aqueous surfactant media. Secondary nucleation during the growth stage was inhibited by carefully controlling the growth conditions, and in particular by using ascorbic acid as a weak reducing agent, that cannot reduce gold salt in the presence of the micelles if the seed is not present. By controlling the growth

conditions in aqueous surfactant media, it was possible to synthesize gold nanorods with tunable aspect ratio.

Phase-transfer is another common method for the synthesis of gold nanoparticles containing non-specific ligand shells through the use of tetraoctyl ammonium bromide (TOAB) as reported by Brust *et al.* [8]. In this method, HAuCl_4 is transferred from the aqueous phase to toluene and subsequently reduced by NaBH_4 in the presence of the phase-transfer reagent to form toluene soluble gold nanoparticles. Although the ability to synthesize a diverse range of core sizes is limited, this method is advantageous in that the resultant nanoparticles can be isolated from solution and the ligand can be exchanged to yield both thiol and amine stabilized nanoparticles. The synthesis of gold nanoparticles using non-specific ligand shells typically yields nanoparticles with large cores. These particles are useful for optical applications, where the strongly enhanced plasmon resonance of the large nanoparticles is useful, and also as tagging agents for biological applications [44]. Also the large nanoparticles produced by these have found utility as precursors in seeded growth reactions.

In this section of the chapter, the simple but elegant ways of generating anisotropic gold nanoparticles using both the seed-mediated and a two-phase technique are reported. In the former technique a structure directing agent in the presence of weak reducing agent is used to produce such nanomaterials. The latter technique primarily involves taking a phase-transfer agent in the organic layer and a metal salt in the aqueous layer. The metal is then reduced using the reducing agent in the presence of a capping agent to produce metal nanoparticles. In both techniques, varied reaction parameters affect the shape and size of the as produced metal nanoparticles.

2.4 EXPERIMENTAL

2.4.1 Synthesis of Gold Nanoparticles by Seed-Mediated Technique

Anisotropic gold nanoparticles were prepared by modifying the previously reported seed-mediated technique by Jana *et al.* [50,51]. Typically, this involves the preparation of

a seed and stock solution before the three step process of synthesizing gold nanoparticles. The seed was prepared by dissolving HAuCl_4 (0.0020 g) and tri-sodium citrate (0.0300 g) in distilled water (20.0 mL) under a nitrogen atmosphere. To this solution a freshly prepared $0.100 \text{ mol dm}^{-3}$ ice cold NaBH_4 (0.60 mL) solution was added. A colour change from light yellow to dark brown was observed indicating the formation of gold nanoparticles. As the seed was allowed to grow, the stock solution containing more metal salt, a structure directing agent, and a weak reducing agent was prepared in a separate flask. The stock solution was prepared by dissolving HAuCl_4 (0.0400 g) and hexadecyltrimethylammonium bromide (HTAB) (5.470 g) in distilled water (150.0 mL), resulting in the formation of a creamy solution. To this, ascorbic acid was added until a white milky solution was formed. This colour change observed was due to the reduction of Au^{3+} to Au^+ . Ascorbic acid is a weak reducing agent and at room temperature, it is not capable of fully reducing the metal ion all the way to the elemental metal. The presence of the structure-directing agent (HTAB) is important in obtaining anisotropic nanoparticles.

2.4.2 Synthesis of Gold Nanoparticles using the Two-Phase Method

The synthesis of gold nanoparticles has been carried out using a two-phase / phase-transfer method in the presence of TOAB. In this typical experiment, TOAB (0.28 g) was dissolved in toluene (8.0 mL) in a 25 mL round bottom flask with stirring. To this solution, 3.0 mL of aqueous gold solution (0.031 g, HAuCl_4) was added under vigorous stirring until the HAuCl_4 was transferred into the organic layer (toluene). When these two solutions of different colours, (light yellow and clear white) were mixed, a reddish colour was formed. After 10 min of mixing, an aqueous PVP (0.100 g) solution was added. The polymer was allowed to further mix with the original solution for about 4 h under stirring. Then a freshly prepared aqueous NaBH_4 solution ($0.100 \text{ mol dm}^{-3}$, 0.60 mL) was injected and this resulted in a colour change from red to purple. Finally, the phases were separated using a funnel. The organic phase was taken for further analysis since it contains the nanoparticles. Further reactions were carried out using different phase-transfer agents, such as tetraethylammonium bromide (TEAB) and hexadecyltrimethylammonium bromide (HTAB).

2.5 RESULTS AND DISCUSSION

2.5.1 Gold Nanoparticles Synthesized by Seed-Mediated Technique

Seeds prepared were between 3 – 5 nm in size and mostly spherical in shape as shown in the TEM image in [Figure 2.22](#). Citrate acted as a capping agent for these nanoparticles which were stable for a few months. The particles were then stored at room temperature before further experimentation, to allow the excess borohydride to be decomposed in water. The synthesis of anisotropic metal nanoparticles was carried out by following a three-seeding protocol, as schematically summarized in [Scheme 2.1](#) under the seed method. Here, two 20 mL conical flasks and one 200 mL conical flask (labeled A, B and C) were taken.

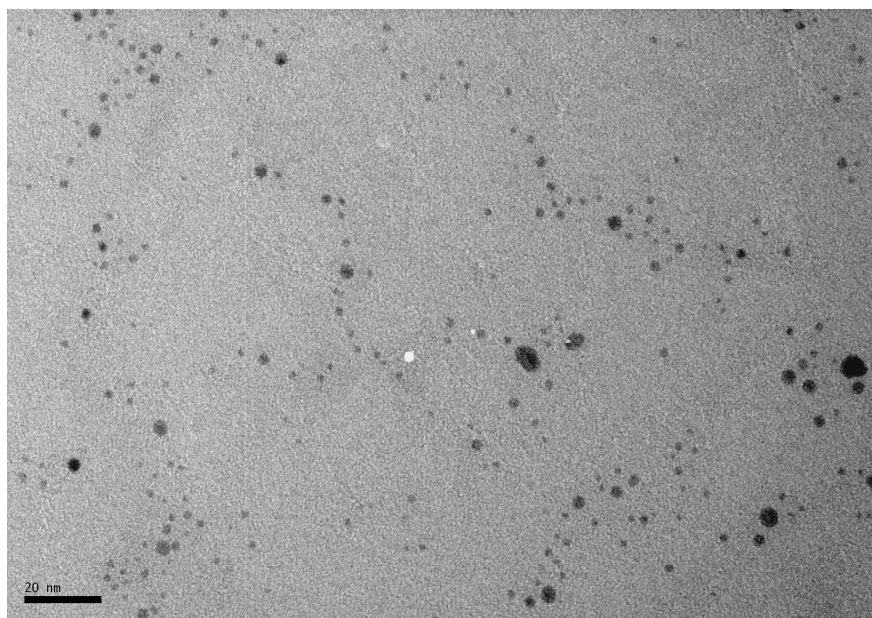


Figure 2.22: TEM image of gold seed.

To these flasks were added 9.0 mL (in flask A and B) and 90.0 mL (in flask C) of stock solution (containing a mixture of 0.0400 g HAuCl_4 , 5.470 g HTAB and 0.100 g ascorbic acid). The stock solution contains Au^+ ions which were not completely reduced to Au^0 by ascorbic acid due to its weak reducing ability. However, further reduction of Au^+ to Au^0 occurred when 1.0 mL of the seed solution was mixed with a solution in flask

A (Step 1). This is confirmed by a rapid development of wine-red colour to the solution in flask A, which was earlier white-milky, thus indicating the formation of gold nanoparticles. When seed particles were introduced in a solution containing Au^+ ions, they act as nucleation centers for catalyzing the reduction of Au^+ to Au^0 on their surfaces. Under normal conditions, introduction of a seed produces particles which are bigger than the seed. At some stage, facets are developed and at this point some of these particles could be directed to grow into nanorods. After about 30 seconds, 1.0 mL of a solution in flask A was added to a solution in flask B (Step 2). This addition resulted in a colour change of this solution to light wine-red indicating the generation of gold nanoparticles. In this step the reduction was slow when compared to step 1. After 30 sec, the content of flask B was transferred to a solution in flask C (Step 3).

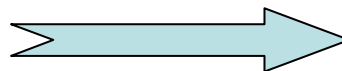
1. Synthesis of seed

0.002 g HAuCl_4 +
0.03 g Trisodium citrate



+

0.6 mL 0.0038 g
Ice-cold NaBH_4



2. Stock solution

0.04 g HAuCl_4 +
5.47 g HTAB

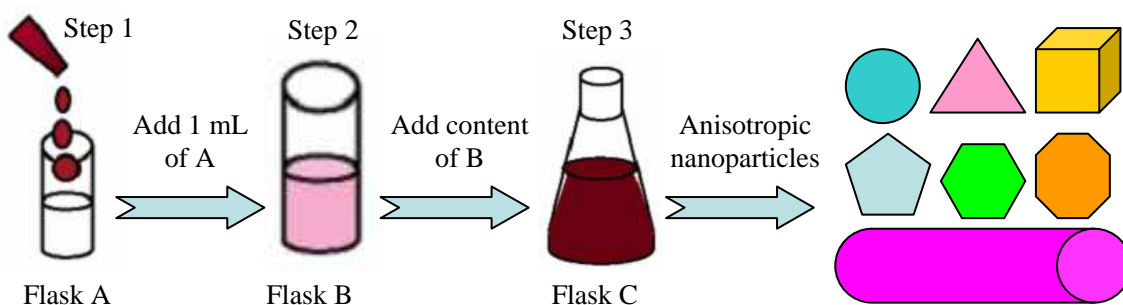


Addition of
ascorbic acid



Reduction of
 Au^{3+} to Au^+

3. Three step protocol for anisotropic synthesis of nanoparticles



Scheme 2.1: Seed-Mediated growth procedure for the synthesis of anisotropic gold nanoparticles.

This transfer resulted in a slow colour change of the solution to wine-red. The colour intensity was observed to increase as the reaction time was increased. In all the above cases, each flask was gently stirred to homogenize the solution. The final solution obtained in step 3, was centrifuged in order to remove excess HTAB before any further analysis. Introduction of the seed to flask A in Step 1, resulted in the formation of gold nanoparticles which were bigger in size than the seed. After an initial period, the seeds have grown into isometric crystals with well-defined Au (111) and Au (100) crystal faces. These enlarged seeds aggregate along these well-defined faces to form penta-twinned species that serve as the starting material for rod growth. [Figure 2.23](#) shows the UV-Visible spectra of the as synthesized gold nanoparticles at the initial and final steps which agree well with the colour changes observed from these solutions.

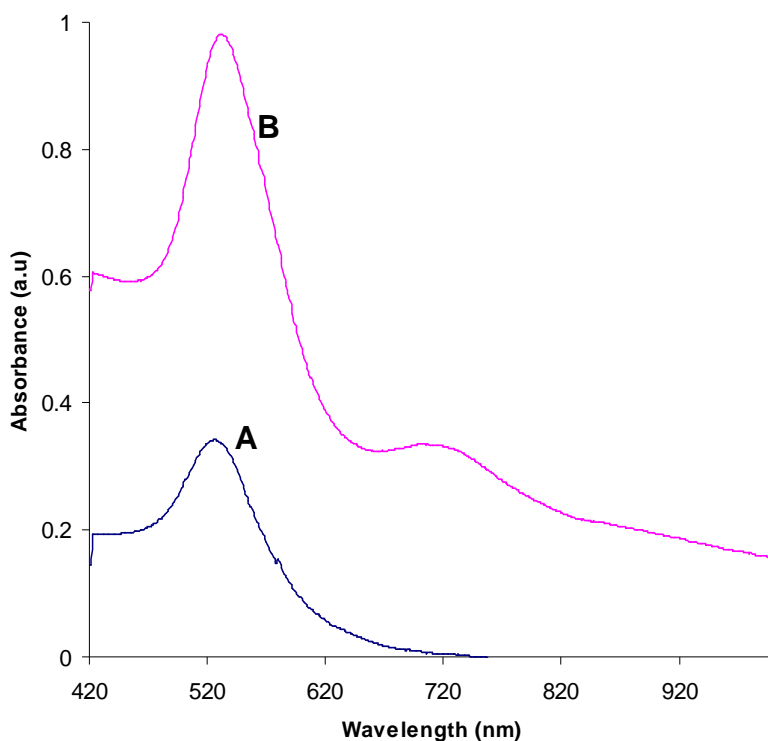


Figure 2.23: UV-Visible spectra of AuNPs: A. at the initial step of seed-method and B. anisotropic AuNPs produced at the final step of the seed-method.

[Figure 2.23A](#) taken at the initial stage (Step 1) shows a single absorption peak at 530 nm which corresponds to the presence of spherical gold nanoparticles. Simultaneous with the twinning events, the surfactant begins to associate and assemble on the Au (100)

faces acting as a directing agent and preventing further growth on the (100) face. As a result, further growth occurs on the Au (111) faces and along the (110) axis, leading to an elongation of the crystal to form nanorods [18,52]. Figure 2.23B shows the UV-Visible spectrum of anisotropic gold nanoparticles produced in the final step (Step 3 – Flask C). From the spectrum two distinct absorption maxima are clearly observed at 535 nm and a broad absorption at longer wavelengths of 650 – 830 nm. These absorption maxima correspond to the transverse plasmon resonance of spherical nanoparticles and the longitudinal plasmon resonance of the non-spherical nanoparticles. From the optical properties it is clearly seen that the nanoparticles produced are larger in size with a mixture of shapes.

Petroski *et al.* [53] have studied the shape distribution of platinum nanoparticles at different stages of their growth as a function of time. They provide two reasonable explanations for the formation and evolution of tetrahedral, truncated octahedral, and cubic shaped nanoparticles, that is: (i) the growth rates vary at different planes of the particles and (ii) particle growth competes with the capping action of stabilizers. A similar scenario might be operative also in this case wherein the introduction of a seed leads to rapid reduction of gold salt on the seed surface. The competitive and preferential binding of HTAB molecules on the surface possibly leads to the generation of faceted spheres which evolve to form anisotropic gold nanoparticles. This formation of anisotropic gold nanoparticles is supported by TEM analysis performed on the as prepared gold nanoparticles. Figures 2.24 and 2.25 shows the TEM images of these nanoparticles before and after centrifugation of the solution. The micrographs taken before centrifugation of the solution are cloudy due to the presence of smaller nanoparticles. The high resolution micrographs in Figure 2.24D and E clearly show some of distinct morphologies (rods and pentahedral) that are observed which are also large in size compared to their seeds of origin.

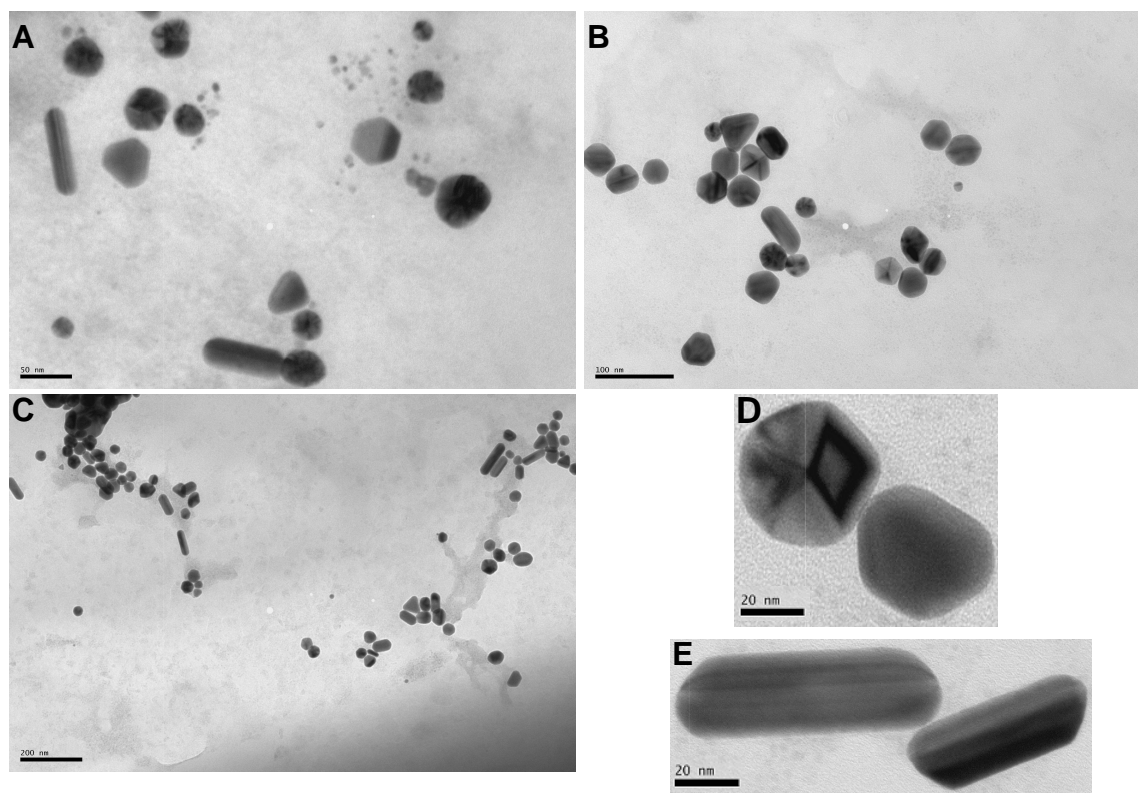


Figure 2.24: A, B, and C are TEM micrographs showing anisotropic AuNPs at different magnification and parts of the grid before centrifugation; D and E are high magnification micrographs.

TEM images taken after the separation of small nanoparticles from the larger ones through centrifugation are shown in Figure 2.25. These images were taken from different regions of the Cu grids at different magnifications. The TEM images clearly show a high percentage of non-spherical nanoparticles, triangles, cubes, pentagons, hexagons and short rods. Gold nanoparticles produced are different in size and shape to the seed particles used, and this confirms that introduction of a seed produces nanoparticles that are bigger than the seed. It is also true that the morphology and size of the nanorods formed depends on the history of the different stages involved in anisotropic shape formation. Murphy *et al.* [54] have investigated this by using (cetyltrimethylammonium bromide) CTAB-capped seed of different sizes to produce nanorods. They also found that the nanoparticles formed were greater than that of the injected seed, suggesting growth on the pre-formed seeds. Comparing this with the current results, it clearly

supports that size, morphology and its subsequent evolution to form anisotropic gold nanoparticles can all be controlled by the initial gold nanoparticle seed size.

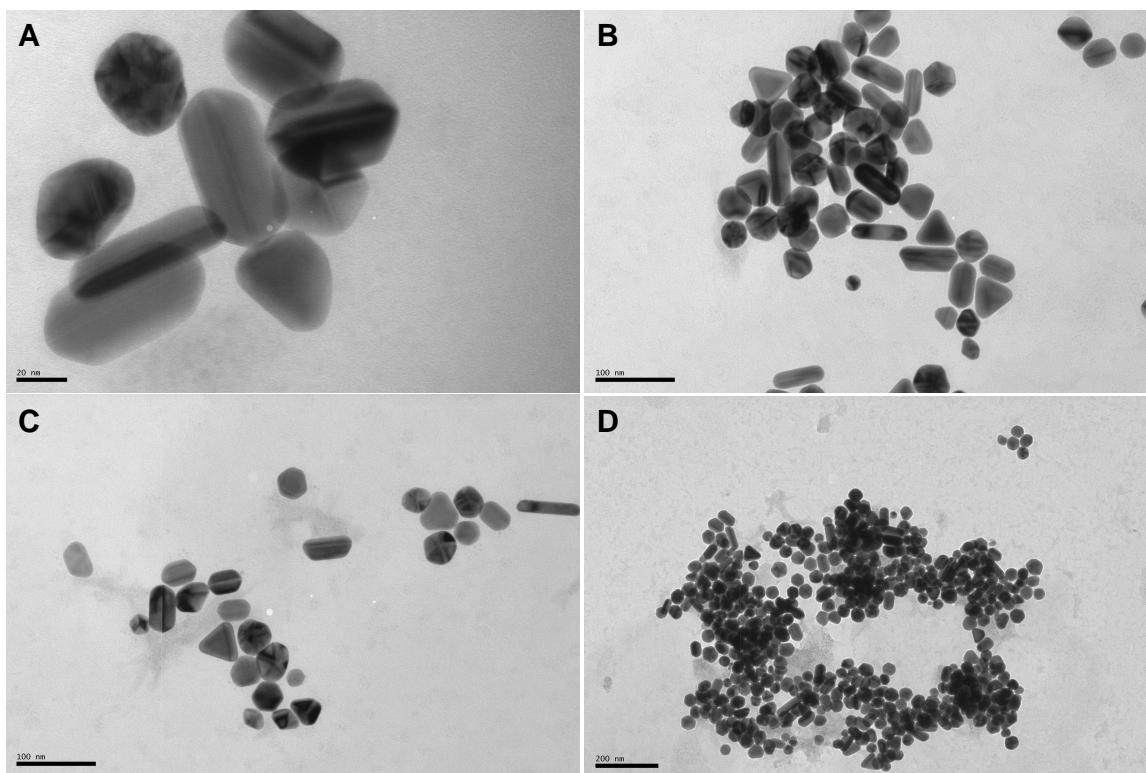


Figure 2.25: A, B, C, and D are TEM micrographs showing anisotropic AuNPs at different magnification and parts of the grid after centrifugation.

Further studies were carried out using other directing agents in the place of HTAB. In these separate reactions, tetraethylammonium bromide (TEAB) and tetramethylammonium chloride (TMAC) were used. Seed nanoparticles used were prepared as mentioned earlier. In these structure-directing agents, the formation of gold nanoparticles under similar conditions was not observed. Murphy *et al.* have also studied that the anion side is important in the making of gold nanoparticles. They found that bromide is crucial in making gold nanorods and cetyltrimethylammonium chloride (CTAC) as a structure-directing agent gives only spheres, while iodide apparently gives a random mixture of shapes. The results reported in this thesis are the nanoparticles of HTAB as a structure-directing agent yielded a random mixture of shaped gold nanoparticles.

2.5.2 Gold Nanoparticles Synthesis using the Two-Phase Method

In this reaction optical and structural properties for gold nanoparticles synthesized using the phase-transfer method are reported. Figure 2.26 shows typical UV-Visible spectra of the as synthesized gold nanoparticles for both TOAB and HTAB. Nanoparticles in TOAB showed absorption at 520 nm, while the HTAB is absorbing at 527 nm.

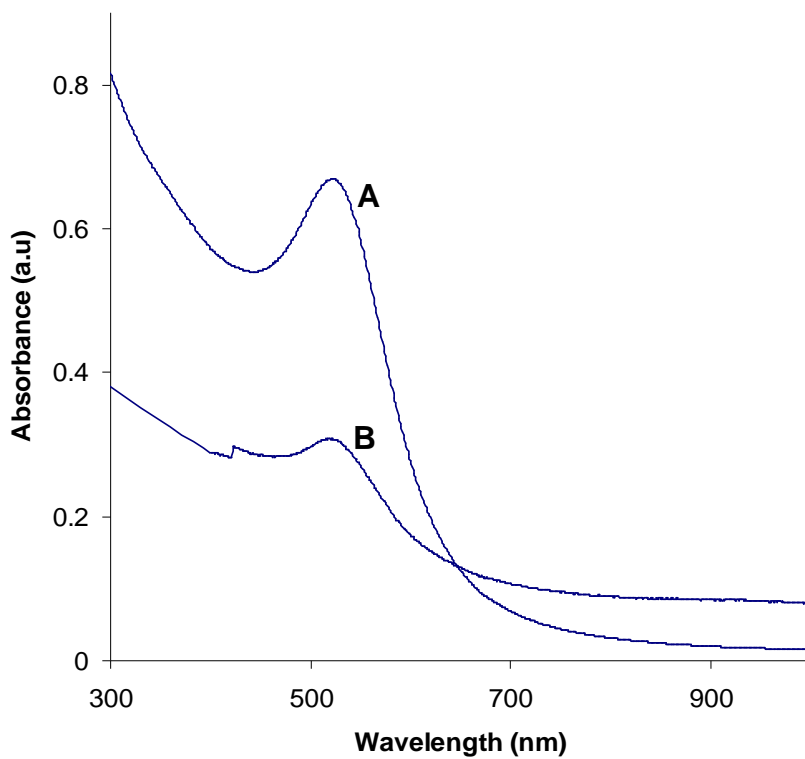


Figure 2.26: UV-Visible spectra of anisotropic AuNPs in A) TOAB and B) HTAB.

This formation of gold nanoparticles was further confirmed by structural analysis through TEM. Figure 2.27 shows the TEM images of these as prepared gold nanoparticles from the above technique taken at different regions of the copper grid. These images are of the metal nanoparticles in which TOAB and HTAB were employed as structure directing agent. Figures 2.27A and B are for TOAB nanoparticles which show well spread monodispersed nanoparticles.

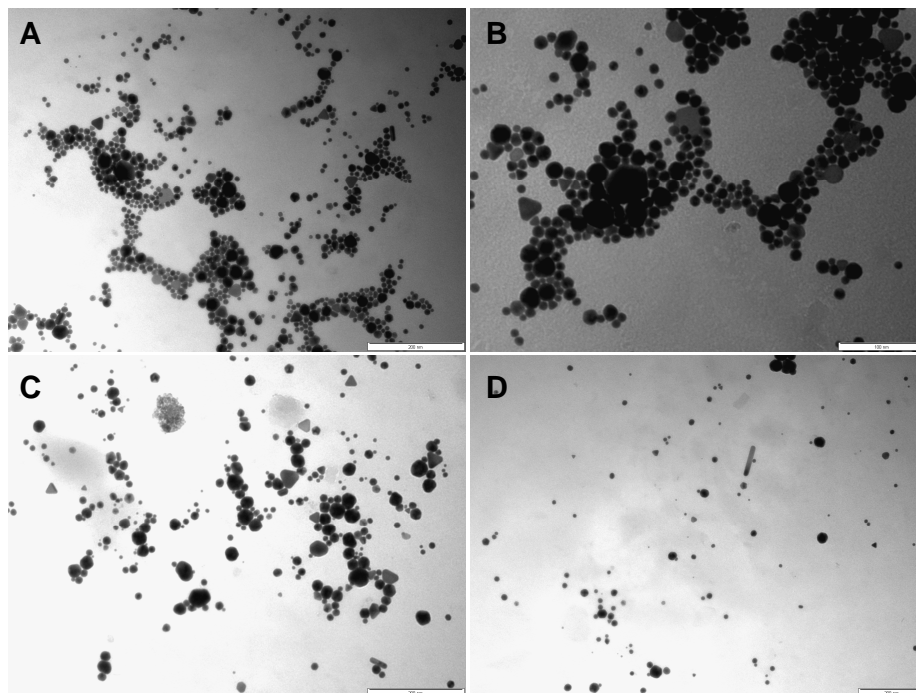


Figure 2.27: TEM micrographs showing anisotropic AuNPs at different magnification and parts of the grid in TOAB (A and B); HTAB (C and D).

Also observed in these images is the dominance of non-spherical shaped nanoparticles, which includes spheres, short rods, pentagon and triangular shaped nanoparticles which are well aligned. Figures 2.27 C and D display nanoparticles in which HTAB was used. Spherical and rod shaped particles are observed in this structure directing agent.

2.6 CONCLUSIONS

This synthesis of gold nanoparticles from various chemical reduction techniques, which have yielded spherical as well as anisotropic shaped nanoparticles was discussed. Different reducing agents were used to reduce Au^{3+} ions to Au^0 to form nanoparticles, stabilized by different polymers which prevented agglomeration. Gold nanoparticles capped either with PVP, PVA or with a mixture of TOPO and ODA were successfully prepared. The average size of the gold nanoparticles capped with TOPO/ODA was 7.29 ± 1.01 nm while most of the PVP capped nanomaterials have sizes in 10 - 40 nm range. The SPR peak for these nanoparticles was consistent with the absorption at 520 and 530

nm, while a red-shift was observed in the presence of ascorbic acid. From the X-ray diffraction data it is clear that the synthesized gold nanoparticles were highly crystalline with fcc cubic structure. The synthetic methods were systematically studied. Chemical reduction offers an opportunity to prepare gold nanoparticles protected with a monodisperse polymer shell. In the seed-mediated method, two distinct absorption maxima were observed while the TEM shows the presence of rods and pentahedral structures. A normal gold absorption around 520 nm and 527 nm was observed for the AuNPs from the two-phase method capped with TOAB and HTAB.

From these studies, it can be concluded that shape control can be achieved by choosing specific reducing, capping, and structure-directing and phase-transfer agents during the growth of nanocrystals. Given that many ions and polymers are now being found to influence nanocrystal growth, it is most likely that there are sufficient empirical data to design rules for growth dynamics. However, in order for this to be done properly, the crystallography of all of these anisotropic shapes need to be determined for different reaction conditions if epitaxial or selective-surface energy arguments are to be made as to which faces grow and which do not. Evidence has been provided in this section for producing well-defined anisotropic gold nanoparticles in an appropriate medium. The technique employed seems to be crucial for size and shape control. The seed-mediated growth was successfully employed to prepare nanocrystalline materials of various sizes and shapes with wide ranging properties. What is noteworthy is that most of the nanoparticles synthesized had the average size within the nanometer range. Furthermore, the method enables one to obtain well-defined shapes, some of which were single crystalline, which is difficult to obtain by any other physical or chemical method. In the chapter 3 the synthesis of anisotropic gold nanoparticles using the UV-irradiation technique is discussed.

2.7 REFERENCES

-
- [1] M.C. Daniel, D. Astruc, *Chem. Rev.*, 2004, **104**, 293.
- [2] F.K. Liu, Y.Y. Lin, C.H. Wu, *Analytica Chimica Acta*, 2005, **528**, 249.
- [3] J. Liu, Y. Lu, *Anal. Chem.*, 2004, **76**, 1627.
- [4] J. Wang, J. Li, A.J. Baca, J. Hu, F. Zhou, W. Yan. D.W. Pang, *Anal. Chem.*, 2003, **75**, 3941.
- [5] J. Turkevitch, P.C. Stevenson, J. Hillier, *Discuss. Faraday Soc.*, 1951, **11**, 55.
- [6] M. Giersig, P. Mulvaney, *Langmuir*, 1993, **9**, 3408.
- [7] M. Faraday, *Philos. Trans.*, 1857, **147**, 145.
- [8] M. Brust, M. Walker, D. Bethell, D.J. Schrifflin, R.J. Whyman, *Chem. Commun.*, 1994, 801.
- [9] J. P. Wilcoxon, R. L. Williamson, R. Baughman, *J. Chem. Phys.*, 1993, **98**, 9933.
- [10] M. Green, P. O'Brien, *Chem. Commun.*, 2000, 183.
- [11] P.R. Selvakannan, S. Mandal, S. Phadtare, R. Pasricha, M. Sastry, *Langmuir*, 2003, **19**, 3545.
- [12] D. Prime, S. Paul, C. Pearson, M. Green, M.C. Petty, *Mater. Sc. and Eng.*, 2005, **25**, 33.
- [13] P.R. Selvakannan, S. Mandal, R. Pasricha, S.D. Adyanthaya, M. Sastry, *Chem. Commun.*, 2002, 1334.
- [14] C.B. Murray, D.J. Norris, M.G. Bawendi, *J. Am. Chem. Soc.*, 1993, **115**, 8706.
- [15] M. Green, N. Allsop, G. Wakefield, P. J. Dobson, J. L. Hutchison, *J. Mater. Chem.*, 2002, **12**, 2671.
- [16] S. Nath, S. Praharaj, S. Panigrahi, S. Kundu, S. K. Ghosh, S. Basu, T. Pal, *Colloids and Surfaces A: Physicochem. Eng. Aspects*, 2006, **274** 145.
- [17] Z. Chen, L. Gao, *Materials Research Bulletin*, 2007, **42**, 1657.
- [18] C.J. Murphy, T. K. Sau, A. M. Gole, C. J. Orendorff, J. Gao, L. Gou, S. E. Hunyadi, T. Li, *J. Phys. Chem. B*, 2005, **109**, 13857.
- [19] T.G. Schaaff, M.N. Shafiqullin, J.T. Houry, I. Vezmar, R.L. Whetten, W.G. Cullen, P.N. First, C. Gutiérrez-Wing, J. Ascensio, M.J. Jose-Yacamán, *J. Phys. Chem. B*, 1997, **101**, 7885.

-
- [20] K.L. Kelly, E. Coronado, L.L. Zhao, G.C. Schatz, *J. Phys. Chem. B*, 2003, **107**, 668.
- [21] A. Taleb, C. Petit, M.P. Pileni, *J. Phys. Chem. B*, 1998, **102**, 2214.
- [22] S. Link, M.B. Mohamed, M.A. El-Sayed, *J. Phys. Chem. B*, 1999, **103**, 3073.
- [23] N.R. Jana, L. Gearheart, S.O. Obare, C.J. Murphy, *Langmuir*, 2002, **18**, 922.
- [24] C. Cretu, E. van der Lingen, *Gold Bulletin*, 1999, **22**, 115.
- [25] Y. Sun, Y. Xia, *Analyst*, 2003, **128**, 686.
- [26] N.R. Jana, L. Gearheart, C.J. Murphy, *Adv. Mater.*, 2001, **13**, 1389.
- [27] S. Kundu, V. Maseshwari, R.F. Saraf, *Langmuir*, 2008, **24**, 551.
- [28] J.M. Petroski, Z.L. Wang, T.C. Green, M.A. El-Sayed, *J. Phys. Chem. B*, 1998, **120**, 3316.
- [29] J.L. Burt, J.L. Elechiguerra, *J. Crystal Growth*, 2005, **285**, 681.
- [30] J.H. Lee, K. Kamada, N. Enomoto, J. Hojo, *J. Colloid and Interface Sc.*, 2007, **316**, 887.
- [31] Y.T. Lee, S.H. Im, B. Willey, Y. Xia, *Chem. Phys. Lett.*, 2005, **411**, 479.
- [32] A.R. Roosan, W.C. Carter, *Physica A*, 1998, **261**, 232.
- [33] I. Washio, Y.J. Xiong, Y.D. Yin, Y.N. Xia, *Adv. Mater.*, 2006, **18**, 1745.
- [34] Y. Sun, B. Mayers, T. Herricks, Y. Xia, *Nano Lett.*, 2003, **7**, 955.
- [35] Y. Gao, P. Jiang, D. F. Liu, H. J. Yuan, X. Q. Yan, Z. P. Zhou, J. X. Wang, L. Song, L. F. Liu, W. Y. Zhou, G. Wang, C. Y. Wang, S. S. Xie, *J. Phys. Chem. B*, 2004, **108**, 12877.
- [36] K. Mihama, Y. Yasuda, *J. Phys. Jpn*, 1966, **21**, 1166.
- [37] Y.K. Du, J.Z. Xu, M. Shen, P. Yang, L. Jiang, *Colloids and Surfaces A: Physicochem. Eng. Aspects*, 2008, **330**, 55.
- [38] S. Chen, H. Yao, K. Kimura, *Langmuir*, 2001, **17**, 733.
- [39] Y. Sun, B. Mayers, T. Herricks, Y. Xia, *Nano Lett.*, 2003, **3**, 955.
- [40] N.R. Jana, L. Gearheart, C.J. Murphy, *J. Phys. Chem. B*, 2001, **105**, 4065.
- [41] J.E. Millstone, G.S. Metraux, C.A. Mirkin, *Adv. Funct. Mater.*, 2006, **16**, 1209.
- [42] F. Kim, S. Connor, H. Song, T. Kuykendall, P.D. Yang, *Angew. Chem., Int. Ed.*, 2004, **43**, 3673.
- [43] Y.G. Sun, Y.N. Xia, *Science*, 2002, **298**, 2176.

-
- [44] F. Hao, C.L. Nehl, J.H. Hafner, P. Nordlander, *Nano Lett.*, 2007, **7**, 729.
- [45] B.M.I. Van der Zande, M.R. Bohmer, L.G.J. Fokkink, C. Schonenberger, *Langmuir*, 2000, **16**, 451.
- [46] T.S. Ahmadi, Z.L. Wang, T.C. Green, A. Henglein, M.A. El-Sayed, *Science*, 1996, **272**, 1924.
- [47] A. Filankembo, S. Giorgio, I. Lisiecki, M.P. Pileni, *J. Phys. Chem. B*, 2003, **107**, 7492.
- [48] K.R. Brown, D.G. Walter, M.J. Natan, *Chem. Mater.*, 2000, **12**, 306.
- [49] W.R. Glomm, *J. Dispersion, Sci. and Technol.*, 2005, **26**, 389.
- [50] N.R. Jana, L. Gearheart, C.J. Murphy, *Chem. Mater.*, 2001, **13**, 2313.
- [51] N.R. Jana, L. Gearheart, C.J. Murphy, *Langmuir*, 2001, **17**, 6782.
- [52] J. Perez-Juste, L.M. Liz-Marzan, S. Carnie, D.Y.C. Chan, P. Mulvaney, *Adv. Funct. Mater.*, 2004, **14**, 571.
- [53] J.M. Petroski, Z.L. Wang, T.C. Green, M.A. El-Sayed, *J. Phys. Chem. B*, 1998, **102**, 3316.
- [54] A. Gole, C.J. Murphy, *Chem. Mater.*, 2004, **16**, 3633.